U.S. Department
of Transportation
Federal Railroad
Administration

Office of Research,
Development and Technology
Washington, DC 20590

Automated Track Change Detection Technology for Enhanced Railroad Safety Assessment

DOT/FRA/ORD-23/13

Report | April 2023

NOTICE

This document is disseminated under the sponsorship of the Department of Transportation in the interest of information exchange. The United States Government assumes no liability for its contents or use thereof. Any opinions, findings and conclusions, or recommendations expressed in this material do not necessarily reflect the views or policies of the United States Government, nor does mention of trade names, commercial products, or organizations imply endorsement by the United States Government. The United States Government assumes no liability for the content or use of the material contained in this document.

NOTICE

The United States Government does not endorse products or manufacturers. Trade or manufacturers' names appear herein solely because they are considered essential to the objective of this report.

REPORT DOCUMENTATION PAGE

Form Approved
OMB No. 0704-0188

1. AGENCY USE ONLY (Leave blank)	2. REPORT DATE	3. REPORT TYPE AND DATES COVERED
	April 2023	Technical Report

4. TITLE AND SUBTITLE
Automated Track Change Detection Technology for Enhanced Railroad Safety Assessment

5. FUNDING NUMBERS
693JJ619C000004

6. AUTHOR(S)
Ryan M. Harrington[1], Arthur de O. Lima[1], J. Riley Edwards[1], Marcus S. Dersch[1], Richard Fox-Ivey[2], John Laurent[2], and Thanh Nguyen[2]

7. PERFORMING ORGANIZATION NAME(S) AND ADDRESS(ES)
University of Illinois at Urbana-Champaign[1]
506 S. Wright St.
Urbana, IL 61801-3620

Pavemetrics Systems Inc.[2]
150 Boulevard René-Lévesque E #1820
Québec, QC G1R 5B1

8. PERFORMING ORGANIZATION REPORT NUMBER
N/A

9. SPONSORING/MONITORING AGENCY NAME(S) AND ADDRESS(ES)
U.S. Department of Transportation
Federal Railroad Administration
Office of Railroad Policy and Development
Office of Research, Development, and Technology
Washington, DC 20590

10. SPONSORING/MONITORING AGENCY REPORT NUMBER
DOT/FRA/ORD-23/13

11. SUPPLEMENTARY NOTES
COR: Cameron Stuart

12a. DISTRIBUTION/AVAILABILITY STATEMENT
This document is available to the public through the FRA website.

12b. DISTRIBUTION CODE

13. ABSTRACT (Maximum 200 words)

The Rail Transportation and Engineering Center at the University of Illinois at Urbana-Champaign and Railmetrics, Inc. evaluated the use of 3D laser scanning, Deep Convolutional Neural Networks (DCNNs), and change detection technology for railway track safety inspections. Researchers evaluated the potential use of these combined technologies to provide value-added inspection data to traditional track inspection methods. The project was conducted between April 2019 and October 2020. Field testing was completed on the High Tonnage Loop at the Transportation Technology Center in Pueblo, Colorado.

The results from this project establish the viability of the combination of 3D laser triangulation technology, coupled with DCNNs and change detection algorithms, to reliably detect and classify a wide variety of track components and conditions that influence the safety of train operations, and to report changes in these features over time with high precision. This technology advances the state-of-the-art in automated track inspection, going beyond the simple pass/fail assessments typical of current inspection approaches. During the test program, it detected a wide range of both small and large changes related to elastic fasteners, spikes, joint bar gaps, joint bar bolting, crosstie skew, ballast level, and ballast fouling.

14. SUBJECT TERMS
3D laser triangulation, artificial intelligence, AI, deep convolutional neural networks, algorithms, change detection, safety, operational efficiency, inspection, technology-augmented human inspection

15. NUMBER OF PAGES
48

16. PRICE CODE

17. SECURITY CLASSIFICATION OF REPORT	18. SECURITY CLASSIFICATION OF THIS PAGE	19. SECURITY CLASSIFICATION OF ABSTRACT	20. LIMITATION OF ABSTRACT
Unclassified	Unclassified	Unclassified	

NSN 7540-01-280-5500
Standard Form 298 (Rev. 2-89)
Prescribed by ANSI Std. 239-18
298-102

METRIC/ENGLISH CONVERSION FACTORS

ENGLISH TO METRIC	METRIC TO ENGLISH
LENGTH (APPROXIMATE)	**LENGTH (APPROXIMATE)**
1 inch (in) = 2.5 centimeters (cm)	1 millimeter (mm) = 0.04 inch (in)
1 foot (ft) = 30 centimeters (cm)	1 centimeter (cm) = 0.4 inch (in)
1 yard (yd) = 0.9 meter (m)	1 meter (m) = 3.3 feet (ft)
1 mile (mi) = 1.6 kilometers (km)	1 meter (m) = 1.1 yards (yd)
	1 kilometer (km) = 0.6 mile (mi)
AREA (APPROXIMATE)	**AREA (APPROXIMATE)**
1 square inch (sq in, in^2) = 6.5 square centimeters (cm^2)	1 square centimeter (cm^2) = 0.16 square inch (sq in, in^2)
1 square foot (sq ft, ft^2) = 0.09 square meter (m^2)	1 square meter (m^2) = 1.2 square yards (sq yd, yd^2)
1 square yard (sq yd, yd^2) = 0.8 square meter (m^2)	1 square kilometer (km^2) = 0.4 square mile (sq mi, mi^2)
1 square mile (sq mi, mi^2) = 2.6 square kilometers (km^2)	10,000 square meters (m^2) = 1 hectare (ha) = 2.5 acres
1 acre = 0.4 hectare (he) = 4,000 square meters (m^2)	
MASS - WEIGHT (APPROXIMATE)	**MASS - WEIGHT (APPROXIMATE)**
1 ounce (oz) = 28 grams (gm)	1 gram (gm) = 0.036 ounce (oz)
1 pound (lb) = 0.45 kilogram (kg)	1 kilogram (kg) = 2.2 pounds (lb)
1 short ton = 2,000 pounds (lb) = 0.9 tonne (t)	1 tonne (t) = 1,000 kilograms (kg) = 1.1 short tons
VOLUME (APPROXIMATE)	**VOLUME (APPROXIMATE)**
1 teaspoon (tsp) = 5 milliliters (ml)	1 milliliter (ml) = 0.03 fluid ounce (fl oz)
1 tablespoon (tbsp) = 15 milliliters (ml)	1 liter (l) = 2.1 pints (pt)
1 fluid ounce (fl oz) = 30 milliliters (ml)	1 liter (l) = 1.06 quarts (qt)
1 cup (c) = 0.24 liter (l)	1 liter (l) = 0.26 gallon (gal)
1 pint (pt) = 0.47 liter (l)	
1 quart (qt) = 0.96 liter (l)	
1 gallon (gal) = 3.8 liters (l)	
1 cubic foot (cu ft, ft^3) = 0.03 cubic meter (m^3)	1 cubic meter (m^3) = 36 cubic feet (cu ft, ft^3)
1 cubic yard (cu yd, yd^3) = 0.76 cubic meter (m^3)	1 cubic meter (m^3) = 1.3 cubic yards (cu yd, yd^3)
TEMPERATURE (EXACT)	**TEMPERATURE (EXACT)**
[(x-32)(5/9)] °F = y °C	[(9/5) y + 32] °C = x °F

QUICK INCH - CENTIMETER LENGTH CONVERSION

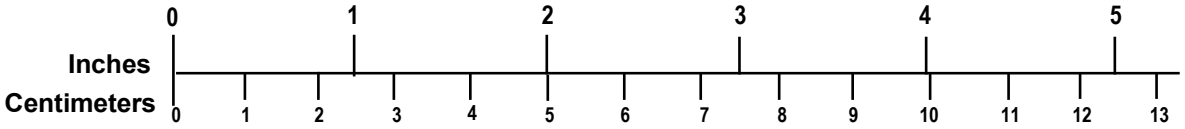

QUICK FAHRENHEIT - CELSIUS TEMPERATURE CONVERSIO

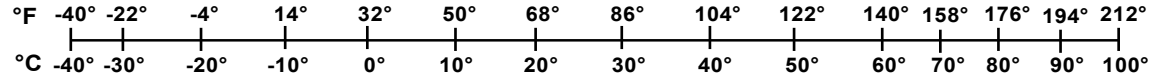

For more exact and or other conversion factors, see NIST Miscellaneous Publication 286, Units of Weights and Measures. Price $2.50 SD Catalog No. C13 10286

Updated 6/17/98

Contents

Illustrations

Tables

Executive Summary

The Rail Transportation and Engineering Center at the University of Illinois at Urbana-Champaign and Railmetrics, Inc. evaluated the use of 3-dimensional (3D) laser scanning, Deep Convolutional Neural Networks (DCNNs), and change detection technology for railway track safety inspections. The objective of this project was to evaluate the potential use of these combined technologies to provide value-added inspection data to traditional track inspection methods. The project was conducted between April 2019 and October 2020. Field testing was completed on the High Tonnage Loop (HTL) at the U.S. Department of Transportation's Transportation Technology Center in Pueblo, Colorado.

This report discusses current track inspection approaches and technologies and compares them with this new track change detection approach. Next, it describes the process for 3D image capture and DCNN training from scans of the HTL, followed by a comparison between the inspection performance of the trained DCNN and human evaluators. Finally, change detection results are presented from the repeat scans of the HTL during the Facility for Accelerated Service Testing program in fall 2019.

The results from this project establish the viability of the combination of 3D laser triangulation technology, coupled with DCNNs and change detection algorithms, to reliably detect and classify a wide variety of track components and conditions that influence the safety of train operations, and to report changes in these features over time with high precision. This technology advances the state-of-the-art in automated track inspection, going beyond the simple pass/fail assessments typical of current inspection approaches. During the test program, it detected a wide range of both small and large changes related to elastic fasteners, spikes, joint bar gaps, joint bar bolting, crosstie skew, ballast level, and ballast fouling.

Given these promising results, the research team recommends future testing with this technology on revenue service track. This would increase sample sizes for features of interest, increase overall accuracy, and present results for other environmental conditions. Additionally, the team recommends the development a condition change index to objectively quantify the impact of observed changes on the strength and performance of the track system and its components.

1. Introduction

The Rail Transportation and Engineering Center (RailTEC) at the University of Illinois at Urbana-Champaign (Illinois) and Railmetrics, Inc. evaluated the use of 3D laser scanning, Deep Convolutional Neural Networks (DCNNs), and change detection technology for railway track safety inspections. The project was conducted between April 2019 and October 2020 and was a continuation of earlier Federal Railroad Administration (FRA)-funded change detection research by Railmetrics. This research is directly applicable to the FRA Track Research Division's strategic priority of developing track inspection technologies that can detect degraded track features before they become in-service failures.

1.1 Background

FRA regulates track inspection intervals based on track class and its corresponding maximum authorized operating speed. Higher track classes correspond to increasing train operating speeds and more frequent track inspection requirements – as often as twice per week for FRA Classes 4 and 5 [1]. Railroads often impose more restrictive inspection practices than FRA's minimum safety requirements to ensure infrastructure resilience. These inspections are typically performed manually by walking track or by riding in hi-rail vehicles. While inspectors often possess a great deal of knowledge and experience, the process is nevertheless subjective, and the logistics and accuracy of performing detailed inspections across the entire track area at hi-rail speeds are very challenging. These challenges have driven the industry to develop machine-based inspection tools which use digital imaging, image processing, and artificial intelligence (AI) to augment human inspections.

To date, several companies have developed machine vision inspection systems. Loram Technologies' (formerly Georgetown Rail) Aurora Xiv system inspects and grades timber and concrete crossties, identifies rail base corrosion, and quantifies ballast levels by capturing light reflected off the track [2; 3]. High-powered xenon lights are employed by ENSCO's track imaging system to illuminate rails, where the reflected light is captured by a set of 2D cameras to identify joint bar cracks [4]. Similarly, bvSys' Railcheck also captures reflected light from light emitting diodes to produce 2D images which are analyzed to locate rail, concrete crosstie, fastener, and ballast level anomalies [5]. MERMEC uses optics in its chord-based Rail Corrugation and V-Cube systems to identify rail corrugations and track level defects through 2D laser profiling [6]. Lastly, Railmetrics' Laser Rail Inspection System (LRAIL) captures 3D profiles and 2D images simultaneously to measure rail geometry and inspect rail surfaces, fasteners, spikes, ballast, and crossties [7]. Most automated inspection technologies are designed for defect location and detection when railway components have reached either a railway maintenance threshold value or an FRA-mandated safety value.

Deep Convolutional Neural Networks (DCNNs) are machine learning programs that use deep learning for image recognition. Over the past 2 decades, these programs have outperformed other pattern recognition methods since they incorporate reinforcement learning to learn and interact with unknown environments [8]. Several studies have paired DCNNs with image capture technology for identifying different features of interest along the railway from 2D images. Chen et al. [9] employed a DCNN to identify defects on catenary system support elements. Similarly, DCNNs have proven effective at detecting other features along the track from 2D images, including rail surface defects [10], fasteners [11], and concrete crosstie cracks [12; 13]. Feature

identification using DCNNs is well established, but there has been minimal research directed toward investigating how DCNNs can be paired with other algorithms to expand their utility beyond binary pass/fail inspections to more sophisticated tasks such as change detection.

Change detection programs automatically identify changes in features over time by comparing new data to a preexisting data. When paired with image recognition software, change detection can locate changes in the track system that would be virtually impossible to detect by traditional human vision inspection. Understanding how track conditions change over time may improve a railroad's ability to effectively conduct preventative maintenance and reduce the occurrence of defects in track.

To explore the benefits of automated track change detection, FRA has sponsored several recent research projects. The first project, conducted by ENSCO, collected and evaluated 2D "before" and "after" images from two independent surveys [14]. ENSCO software could identify alterations in fastener condition, crosstie condition, and rail surface in the 2D track images [14]. The second was conducted by Railmetrics in two parts. The first part was a proof-of-concept effort, and the second part further developed the LRAIL prototype [15; 16]. LRAIL technology was used to evaluate datasets captured 2 months apart on Amtrak's Northeast Corridor. The prototype system could identify changes to crosstie skew angle, fasteners, joint gap, joint bar bolting, and ballast levels with high repeatability – more than 95 percent [16].

1.2 Objectives

The objective of this project was to continue the development and testing of LRAIL-based change detection through testing on the U.S. Department of Transportation's Transportation Technology Center's (TTC) High Tonnage Loop (HTL) during the fall 2019 cycle of Facility for Accelerated Service Testing (FAST) train operations. Project goals included conducting multiple HTL track surveys with LRAIL, establishing ground truth datasets with human inspectors for comparison to sensor-collected data, testing and refining the algorithms that interrogate the raw data to identify and classify various track features, and isolating track feature changes over time using change detection algorithms. The project was designed to validate the accuracy and precision of the system in comparison with human inspection results, to refine and expand the system's feature detection and classification capabilities through testing and training on the wide variety of components and systems installed on the HTL, and to demonstrate the ability of the system to detect changes in the track components and systems over time and tonnage.

The research team established a conservative, 75 percent performance target for agreement between the system outputs and the human evaluator for the following track conditions:

- Ballast conditions (e.g., fouled, too little ballast, excessive ballast)
- Fastener conditions (e.g., multiple missing fasteners in a stretch, multiple poorly aligned fasteners in a stretch)
- Concrete crosstie conditions (e.g., significant cracking, large chips, excessive skew)
- Timber crosstie conditions (e.g., surface cracking and other deterioration, excessive skew)

The team developed a set of change-detecting sensitivity targets to evaluate system performance against metrics created through consultation with the FRA, Amtrak, Canadian National Railway (CN), and BNSF Railway (BNSF) (Table 1).

Table 1. Regions of Interest for Change Detection

Region of Interest	Reporting Metric
Shoulder ballast	Significant changes in average level relative to top of rail within the crib and shoulder areas, or along a stretch of track **(a change ≥ 30% in average height (less ballast compared to the last run) for an individual crib or ≥ 10% in area for ≥ 3 m)**, changes in fouling (presence of non-ballast materials), changes in the presence of surface water or moisture **(a change in affected area ≥ 0.15 m^2)**
Crib ballast	Significant changes in average level relative to top of rail **(a change ≥ 10% in volume or area in a single crib)**, changes in fouling (presence of non-ballast materials), changes in the presence of water or moisture **(a change in affected area ≥ 0.15 m^2)**
Field and gauge-side fastener areas	Significant changes in present fastener counts per km as a percentage **(± 1%)**, significant changes in the position of multiple fasteners **(≥ 10 mm for three consecutive fasteners in the same position along the same rail)**
Crosstie ends and centers	Significant changes to individual ratings of crossties per km **(≥ 10% change in any crosstie rating category)**, significant changes to skew angle of multiple crossties (**at least 3 consecutive crossties with an increase ≥ 2 degrees per 1 km)**
Joint bars	Significant changes to joint bolting **(one or more missing bolts for any given bar)** and joint bar gap **(≥ 2 mm change in gap between rails)**

1.3 Overall Approach

The major phases of the project included field data collection to capture LRAIL scan data and human ground-truth surveys – followed by the preparation of training data, DCNN training, evaluation of the performance of the trained DCNN, and finally the automated detection of changes in track conditions using output data from the trained DCNNs as inputs (Figure 1).

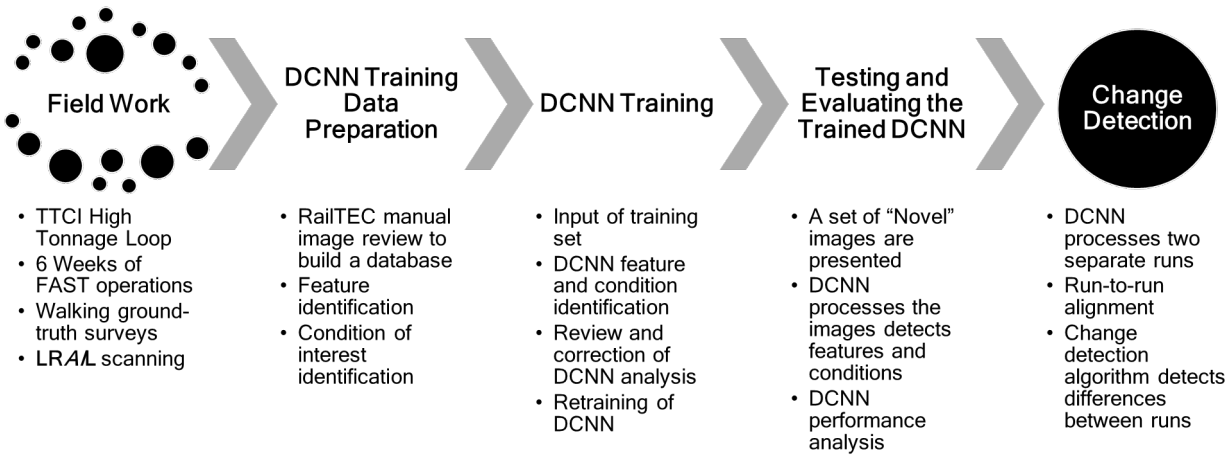

Figure 1. Project Execution Flow Chart

Railmetrics and Illinois divided project responsibilities based on academic expertise and prior research experience. Amtrak, BNSF, and CN served as industry partners by sharing concerns

about various features of interest to aid in project prioritization. The roles of all project partners are shown in Table 2.

Table 2. Roles and Responsibilities

Project Partners	Responsibility
University of Illinois	Provide expert opinion on demanding service environments and types of features to identify. Operate sensors in the field and regular transmission of collected data to Railmetrics. Manually review captured data to build a database of features for training DCNN. Evaluate DCNN classification performance.
Railmetrics, Inc.	Design and fabrication of sensor mounting system. Install and calibrate sensors. Configure and train the DCNN. Process the test data. Generate change detection results.
Amtrak, BNSF and CN	Provide expert opinion on track component features and areas of concern. Prioritize and select features of interest.

1.4 Scope

This report documents field data collection and data analysis efforts directed at the development of an automated track change detection system. The scope of this report includes a description of the measurement system, data processing methods, and detailed results from the collected data.

1.5 Organization of the Report

This report is organized into seven sections, including this introduction. Section 2 documents the field data collection efforts. Section 3 provides a detailed review of DCNN development and validation. Section 4 describes the DCNN alignment process necessary for automated change detection. Section 5 contains the automated track change detection results for the features described in Table 1. Section 6 presents the project conclusions, and Section 7 provides recommendations for future research.

2. Field Data Collection

The team completed field activities at TTC between September 10, 2019, and October 23, 2019. This period overlapped the fall 2019 FAST train operating schedule, with LRAIL scans and human inspections during the day and FAST train operations at night. The first day of testing produced five scans of the HTL track, yielding one dataset for DCNN training and another dataset for DCNN testing. In addition, the team completed a walking inspection of the HTL to establish ground-truth data for DCNN performance training and validation. There were six separate deployments over the test period, each resulting in two or more scans of the HTL in the forward and/or reverse direction, for a total of 35 HTL scans.

2.1 Test Site Characteristics

The 2.7-mile (4.3-km) HTL at TTC is home to FAST train operations. The FAST program is designed to accumulate high traffic tonnage quickly compared to typical revenue service operations on a Class I railroad [1] (Figure 2). On average, each week of FAST operations yielded 8 million gross tons (MGT) of service load, with a total of 57 MGT accumulated during the field test period. The HTL contains a wide variety of track components and systems – an important benefit for this project. The HTL provided a unique opportunity to train and test the system to detect and classify a wide variety of features of interest including tie plates, ballast, spikes, various elastic clip types, and a combination of roughly 10,000 timber and concrete crossties. The high component wear rate from the FAST operations yielded quantifiable changes in feature conditions after each week of FAST operation, shortening the project's schedule.

Figure 2. Satellite View of TTC's High Tonnage Loop in Pueblo, Colorado

2.2 Ground Truth Walking Inspection

RailTEC completed a walking ground-truth inspection during the first deployment, prior to the start of FAST operations, to establish the human inspection data from which to test and train the DCNN outputs. Each track feature of interest was labeled, once per crosstie, for HTL sections 1 to 3, 5 to 9, and 23 to 33. In total, approximately 7,500 crossties were inspected for 15 unique features (Figure 3).

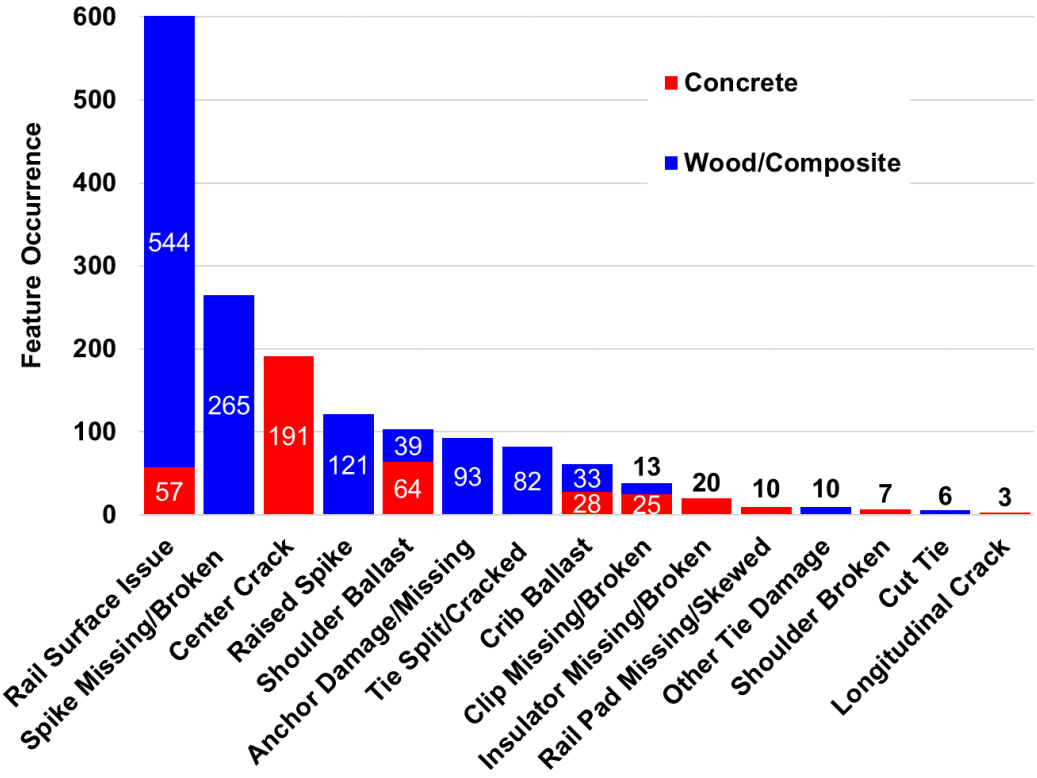

Figure 3. Summary Data from HTL Human Inspection

2.3 LRAIL Data Collection

The team captured 3D scan data of the track using Railmetric's LRAIL system mounted on a hi-rail test trailer pulled by a hi-rail truck (Figure 4).

Figure 4. Hi-rail Truck Pulling Test Trailer Equipped with LRAIL System

The LRAIL sensors project high-frequency (up to 28,000 Hz) laser lines across the track bed, while synchronized cameras use custom filters to capture images of each projected line. Software automatically compiled and merged successive lines from the left and right camera views into a continuous 3.6 m (11.8 ft)-wide image of the track bed.

An optical encoder mounted on a rear wheel of the hi-rail trailer measured vehicle speed. The system captured track images every 2 m (6.6 ft.) along the track. Additionally, a blended inertial navigation system (GPS coupled with an inertial measurement unit) captured the test trailer's latitude, longitude, and elevation, which was also integrated into each 3D profile.

The resulting dataset contained geo-referenced 2D intensity and 3D range data with a longitudinal, transverse, and vertical resolution of 1 mm by 1 mm by 0.1 mm (0.039 in. by 0.039 in. by 0.0039 in.) [16]. The 2D intensity data and the 3D range data are shown in Figure 5. These data were combined to form a continuous track profile (Figure 6).

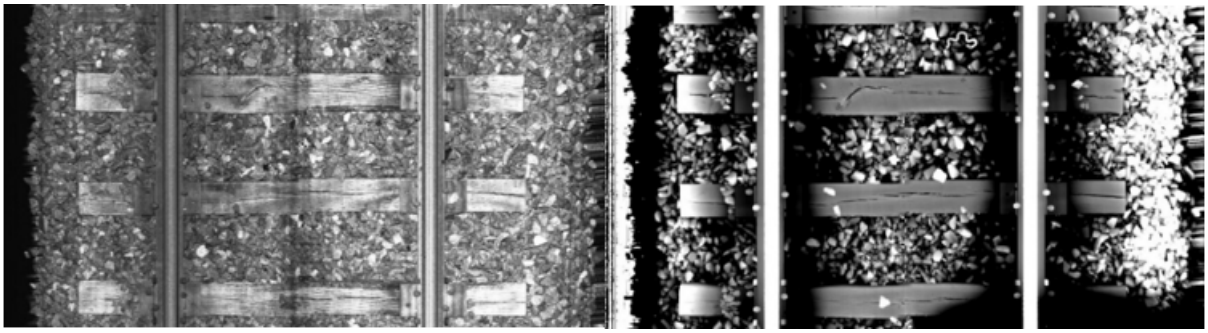

Figure 5. Images from System, 2D Intensity (Left) and 3D Rectified Range (Right)

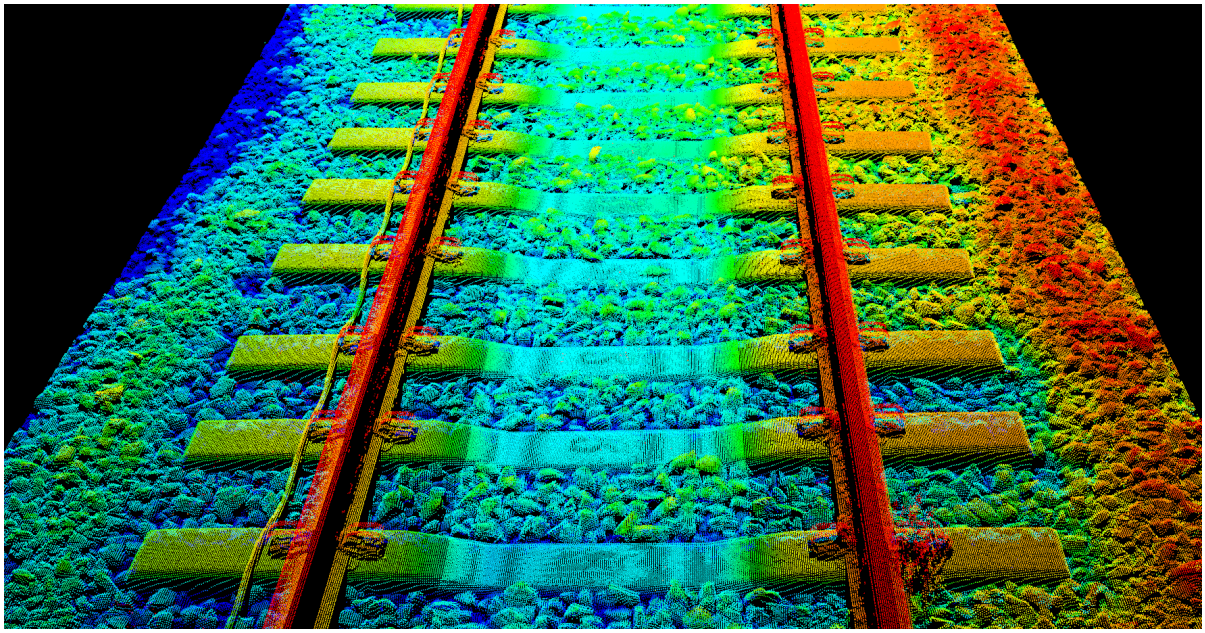

Figure 6. Colorized Combination of Intensity and Range Imaging (LAS File)

3. DCNN Training and Testing

3.1 Configuration and Application of the DCNN

Railmetrics' DCNN consists of a multilayer Region Proposal Network (RPN) and a multilayer classifier network based on fast, region-based, convolutional, neural network architecture. The output layers of both the RPN and the classifier network are softmax and regressor classifiers.

In context of this project, the DCNN was used as a pre-processing tool in advance of the ultimate step of change detection. The function of the DCNN was to accurately and repeatably (1) detect railway features of interest, and (2) classify them in ways that created meaningful data for subsequent change detection. For example, training for elastic fasteners included the detection of both missing and present clips and the further classification of present clips as properly installed, loose, damaged, or covered. Doing so permitted subsequent change detection over a variety range of classifications (e.g., missing to present, present to loose, etc.).

The accuracy and repeatability of the DCNN outputs directly influence the accuracy and repeatability of the automated track change detection process. Training the DCNN to properly identify and classify features of interest was an important first step in this project.

3.2 DCNN Training Data Preparation

The team selected the second inspection run from the first deployment as the training dataset, as it captured the full length of the HTL, and it was time-aligned with the human ground-truth walking inspection. This training set contained 3,800 images: 1,900 2D intensity images and 1,900 3D range images.

The first step of the training process employed the automated analysis of the training dataset using an existing DCNN which had been partially trained during prior projects. The objective was to create a dataset wherein the shortcomings of the preliminarily trained DCNN could be manually reviewed and marked by a human evaluator to create an efficient feedback loop for improving the algorithms.

The second step involved an image-by-image review of the initial results from the DCNN and marking features the DCNN either did not detect or did not properly classify (Figure 7).

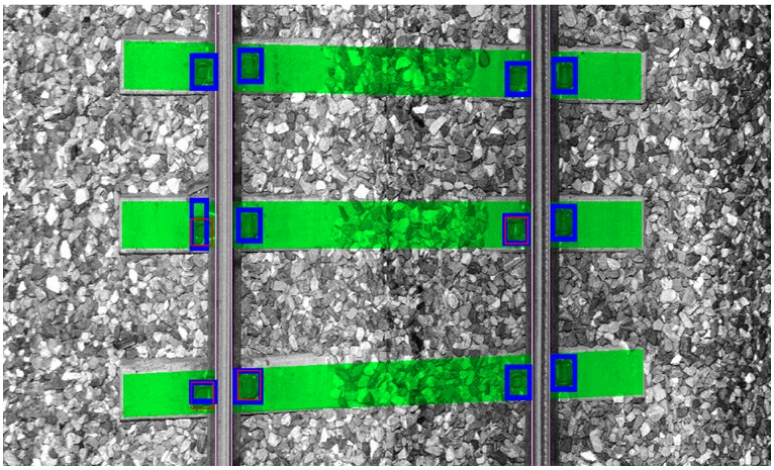

Figure 7. Intensity Image Showing DCNN-Detected Bounding Boxes (Blue) and Human Review Correction Bounding Boxes (Red)

Marked features included tie plates, missing spikes, high spikes, missing and damaged clips, joint bars and joint gaps, damaged crossties, and rail surface defects. The research team used the ground-truth inspection data during this task.

This process effectively reproduced the human evaluator's inspection in a digital format with the exact pixel position of each feature located along with the correct feature classification information in both 2D intensity and 3D range data.

3.3 DCNN Training

The DCNN training process used the manually labeled intensity and range datasets from the training data preparation phase as an input. In total, three rounds of training and validation were repeated, with more than 1.2 million epochs (a complete cycle through the training images) completed in each round.

The team trained the DCNN to detect both the presence and the absence of track features. For features present, the DCNN was further trained to classify each feature to include additional metadata. For example, the DCNN detected both missing and present clips. For present clips, the DCNN classified the condition of the clip – properly installed, loose, damaged, or covered (obscured image). Similarly, the DCNN detected and classified tie plates (type, covered status, missing spike status), spikes (height status), crossties (material, tie grade), joint bars (bolt count), and joint gaps (width measurement). The training process for these features was representative of the training process for all other track features.

3.3.1 Training Example: Elastic Fasteners (Clips)

The DCNN used prepared training images containing examples of each fastener type (e.g., e-Clip) as well as each fastener classification information (e.g., loose) to detect and classify elastic fasteners.

Elastic fastener training included: e-clips, PR clips, Safelok clips (including Safelok I and III), Skl tension clamps, and Pandrol Fastclips. While other clip types were present in the HTL, these five types comprised most of the data and they represent most of the systems currently used in North America. DCNN training for absent fastener detection required training images depicting both standard installations, with four fasteners per tie, and unusual scenarios such as the "dog bone" crosstie shown in Figure 8**,** containing six clip positions per tie.

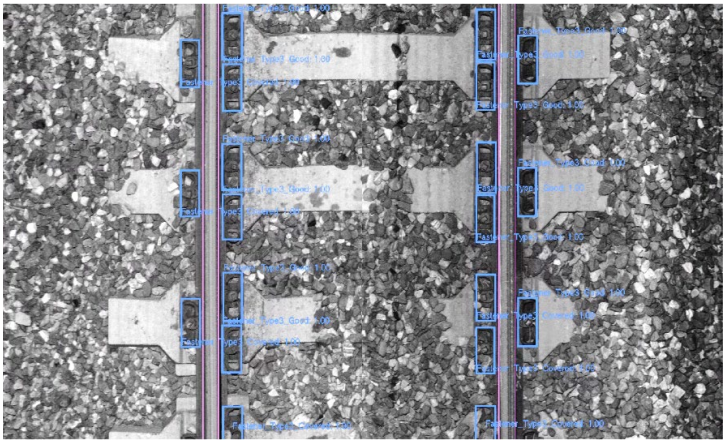

Figure 8. "Dog Bone" Crosstie with 6 Skl Tension Clamp Installation Positions

3.3.2 *Training Example: Spikes*

DCNN spike training included detecting both the presence and the absence of spikes and their classification. Spikes were classified as properly installed, high, or broken (missing head). In addition, the DCNN recognized and reported tie plate spiking patterns.

The system compared spiking patterns between left and right rails and between adjacent crossties. Crossties with mismatched patterns between left and right rails, or ties with spiking patterns that did not match the patterns of proceeding and/or following crossties, were classified as missing spike(s) (Figure 9).

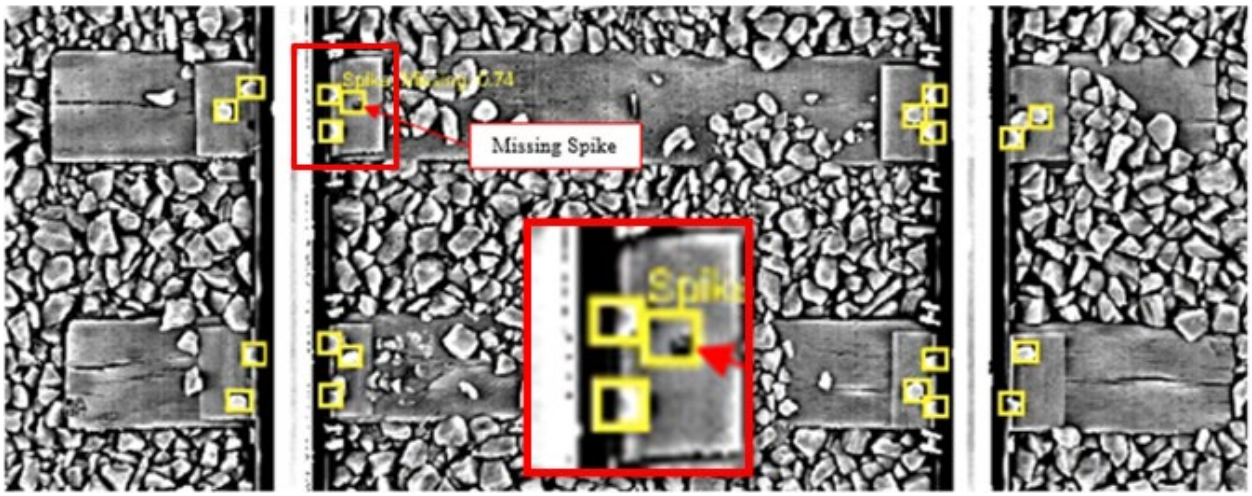

Figure 9. Missing Spike Detected since the Surrounding Tie Plates Have Had 5 Spikes

3.4 Managing and Evaluating the Progress of DCNN Training

TensorFlow Core (open source code for machine learning) managed and monitored training performance during each epoch, or training cycle. Performance was tracked in terms of precision and recall of the DCNN:

- Precision: Indicates the level of false positives which the DCNN generated – or the tendency to report a condition as true when it is false. Precision is calculated as the proportion of true positives to the sum of true positives and false positives.
- Recall: Indicates the level of false negatives which the DCNN generated – or the tendency to report a condition as false when it is true. Recall is calculated as the proportion of true positives to the total number of true positives and false negatives.

The overall performance of the DCNN was evaluated by plotting precision against recall and calculating the area under the curve. The result is expressed as mean average precision loss (mAP Loss), a metric for the general level of algorithm error. Thus, mAP loss achieved for each round of training was used as an indicator of the overall effectiveness and progress of training. Lower mAP loss values indicated higher performance.

The scalars dashboard in TensorBoard recorded mAP loss across each training aspect (feature detection and feature classification) with the progress of each plotted using a different color (Figure 10).

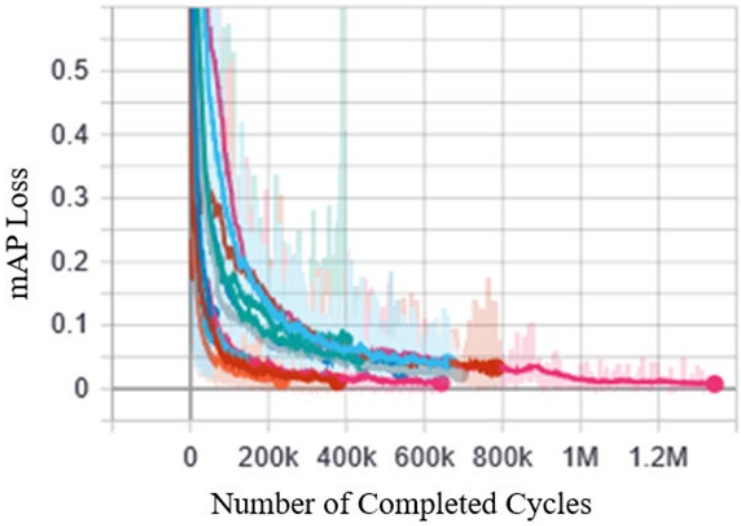

Figure 10. Improvement of DCNN Performance through Training

At the start of the training cycle (e.g., cycles 0–10,000) the general level of error (mAP Loss) for the DCNN was high across all training aspects. After additional training cycles, the mAP loss approached zero, indicating a reduction in DCNN model error and a successful training approach (low false positives and low false negatives). Approximately 1,350,000 training cycles were required in each round of training before the mAP error approached a zero level (high performance) (Figure 10).

Following each round of training, the newly trained DCNN models were implemented into the railway inspection software to automatically process a complete inspection run. This was the technique used to evaluate the performance of the improved models using non-training (new) data (Figure 11). Three rounds of training and model testing were completed before the DCNN models were declared ready for a formal performance evaluation.

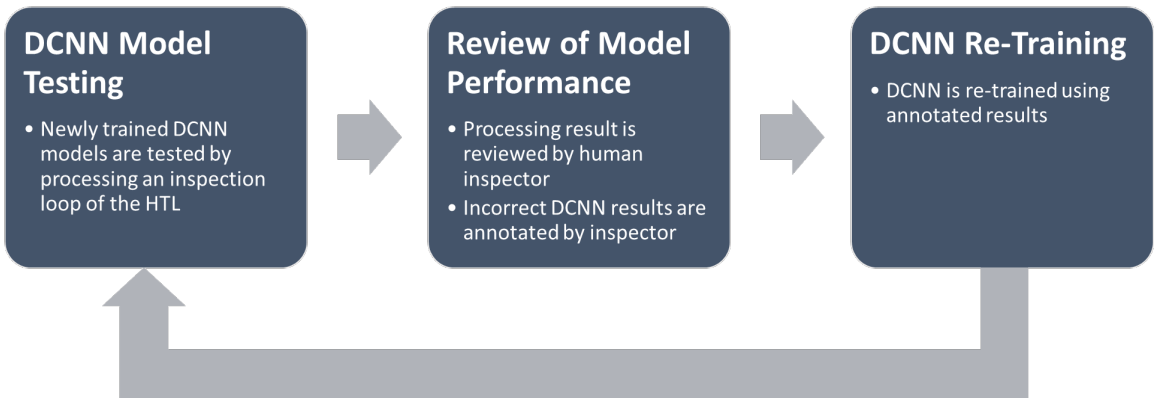

Figure 11. DCNN Training and Evaluation Cycle

3.5 Comparing the Trained DCNN to a Human Evaluator

The performance of the fully trained DCNN was evaluated by comparing DCNN outputs to those generated by a human evaluator. The evaluation used two new datasets. The first dataset was selected from the initial field deployment, and the second was selected from the final field deployment. The rationale for selecting datasets from both the start and end of the field work was to maximize the differences between the datasets due to track degradation from FAST operations.

Each dataset was processed using the trained DCNN to detect and classify railway features. A human evaluator then manually reviewed each DCNN detection and classification result to generate statistics on the trained DCNN's sensitivity (Equation 1), specificity (Equation 2), and percent agreement (Equation 3) [18].

$$Sensitivity = \frac{Feature\ Present}{Feature\ Present + Type\ 2\ Error} * 100\% \quad (1)$$

$$Specificity = \frac{Feature\ Absent}{Type\ 1\ Error + Feature\ Absent} * 100\% \quad (2)$$

$$Percent\ Agreement = \frac{Feature\ Present + Feature\ Absent}{Feature\ Present + Type\ 1\ Error + Type\ 2\ Error + Feature\ Absent} * 100\% \quad (3)$$

The values for the performance metrics are compared to summarize DCNN and human evaluator results in a confusion matrix (Figure 12**)**. The figure also provides example results from the most common type of rail fixation encountered on the HTL, standard cut spikes. In each matrix, green-shaded cells represent agreement between the DCNN and the human evaluator – for either presence or absence of a feature – and peach represents conditions of disagreement.

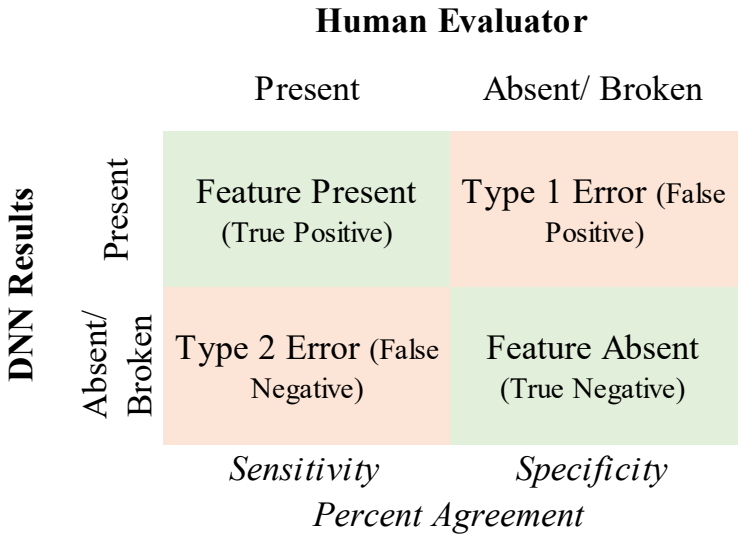

Figure 12. Generalized Confusion Matrix for DCNN Evaluation

Confusion matrices, below, report the results for all features. First, Figure 13 details feature detection quantities based on feature type and the agreement classification between the DCNN and the human evaluator.

Figure 13. Performance Evaluation of DCNN Feature Identification for Novel Datasets

4. Processing DCNN Outputs to Detect Change

Following the successful validation of the DCNN's performance, the research team moved on to the task of change detection. The change detection process can be broadly summarized into three steps: DCNN processing of individual runs, run-to-run alignment, and execution of change analysis (Figure 14).

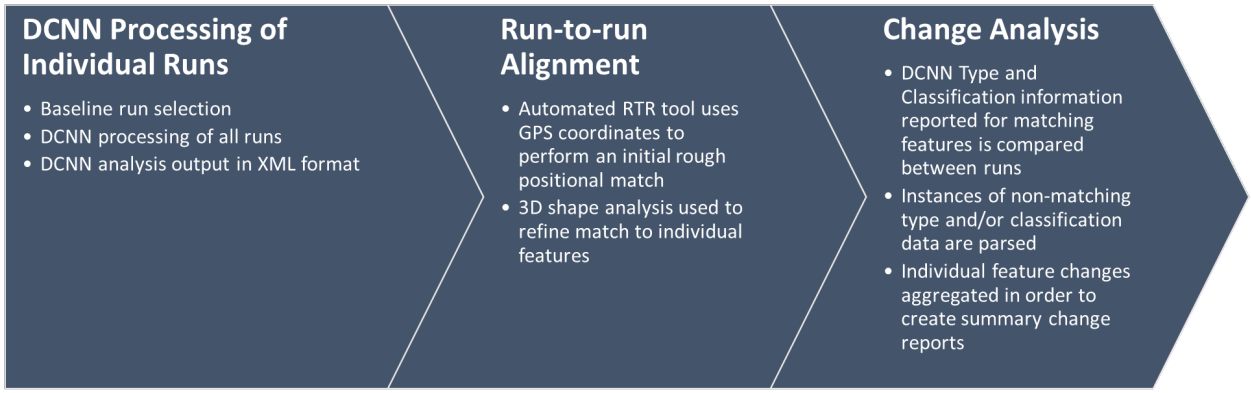

Figure 14. Change Detection Process Flow

4.1 Dataset Selection and DCNN Processing

A single dataset was selected from each of the 7 weeks of field operations to provide a snapshot of the changing HTL track conditions throughout the FAST operating period. Next, the validated DCNN processed each of the datasets to provide a rich dataset of detected and classified features to be analyzed for change detection. The earliest dataset was selected to act as the baseline condition for change reporting against the other six inspection runs. The comparison datasets for the change detection process were:

1. September 10 vs. September 23
2. September 10 vs. October 3
3. September 10 vs. October 7
4. September 10 vs. October 14
5. September 10 vs. October 23

The DCNN processing outputs were a geo-referenced XML report, JPEG images, and 3D files (LAS) generated continuously on a 2-meter basis for the entire length of track. The XML files contained the DCNN geo-referenced detection and classification results which were compared between runs to detect changes.

4.2 Run-to-Run Alignment

The run-to-run alignment process ensured the DCNN processing results pertaining to features from one run could be directly compared to the DCNN processing results for a second run (Figure 15).

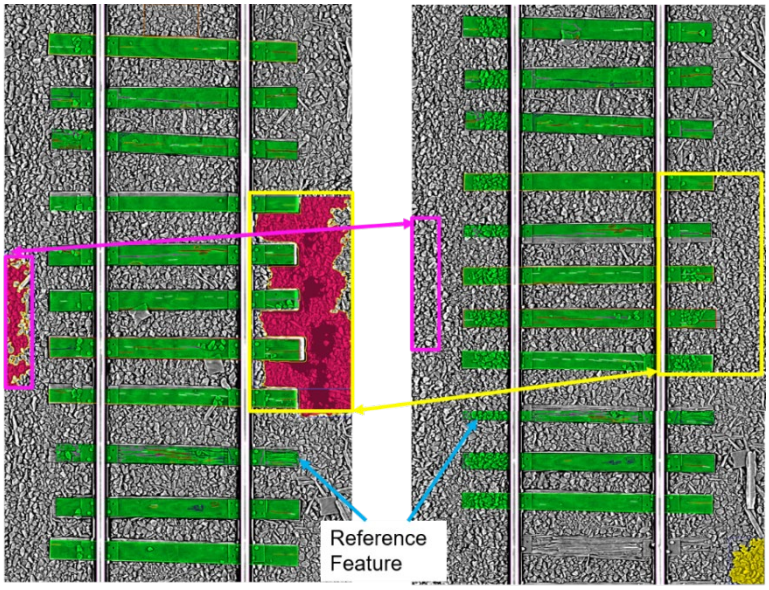

Figure 15. Automated Run-to-Run Alignment

The alignment process was fully automatic. First, the algorithm used GPS coordinates (longitude, latitude, and elevation) stored in the DCNN XML output files from each run to obtain a rough positional match between the two sets of files, within approximately 1 m. Then the process matched individual DCNN-detected features from each run to allow for a feature-to-feature comparison to detect changes. The feature matching used 3D shape analysis to first select a crosstie present in both runs. Finally, from the preliminary match, the algorithm worked outward, using 3D analysis on a variety of railway components, including tie plates, fasteners, and adjacent crossties, to confirm the positional match between runs. The result was a crosstie-by-crosstie match between runs, allowing for the development of change statistics on a crosstie-by-crosstie basis.

5. Automated Track Change Detection Results

The automated change detection algorithm compared DCNN-reported feature and classification data to flag differences between the runs. These findings were then aggregated and summarized in XLS file format to provide change metrics for further evaluation and reporting.

Change reports were generated for a range of track-related features, including:

1. Ballast height
2. Ballast fouling
3. Crosstie skew
4. Crosstie condition
5. Joint bar (and welding strap) bolting and joint gap
6. Elastic fastener inventory
7. Spike height

The following sections describe the change detection results for each feature type.

5.1 Ballast Height Change Detection

Run-to-run comparisons of the mean level of ballast material present in the crib (red) and shoulders (yellow) over 1 m of track to isolate changing ballast levels, (Figure 16).

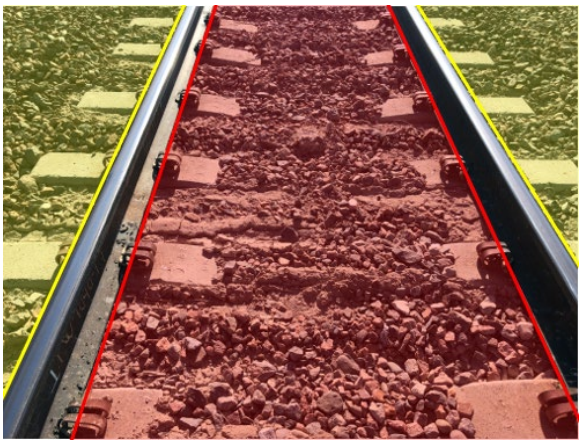

Figure 16. Ballast Height Measurements Locations for Shoulders (Yellow) and Crib (Red)

Ballast level was measured as the absolute distance between the planer surface of the top-most point on each rail and the mean height of the ballast surface (Figure 17). A negative value implies an increase in ballast level since the absolute distance between the rails and the ballast surface decreased. Conversely, a positive value indicates a decrease in ballast height.

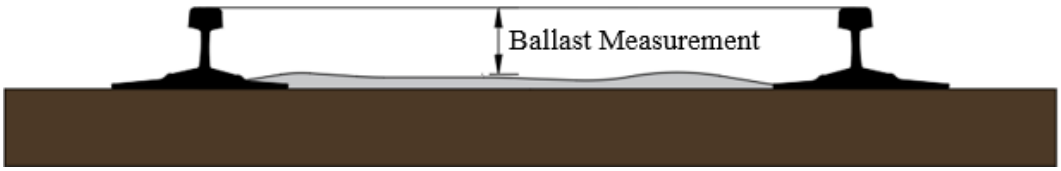

Figure 17. Ballast Height Measurement between Ballast and Rails

Figure 18, Figure 19, and Figure 20 present the run-to-run comparisons between three deployments: September 10 versus September 23, September 10 versus October 3, and September 10 versus October 23 – for the left shoulder, crib, and right shoulder, respectively. The difference in each ballast height measurement is plotted on the Y-axis and the location for each comparison are plotted on the X-axis. The portion of the track between LRAIL section numbers 260 and 360 contained a confidential experiment, thus no data were captured in this region.

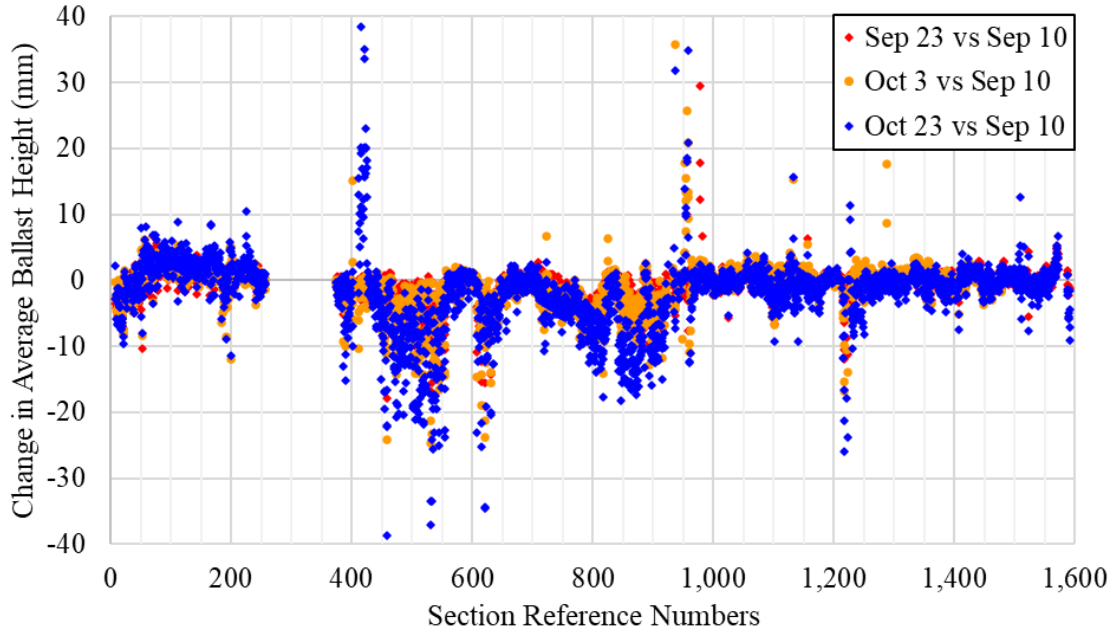

Figure 18. Left Shoulder Ballast Height Changes

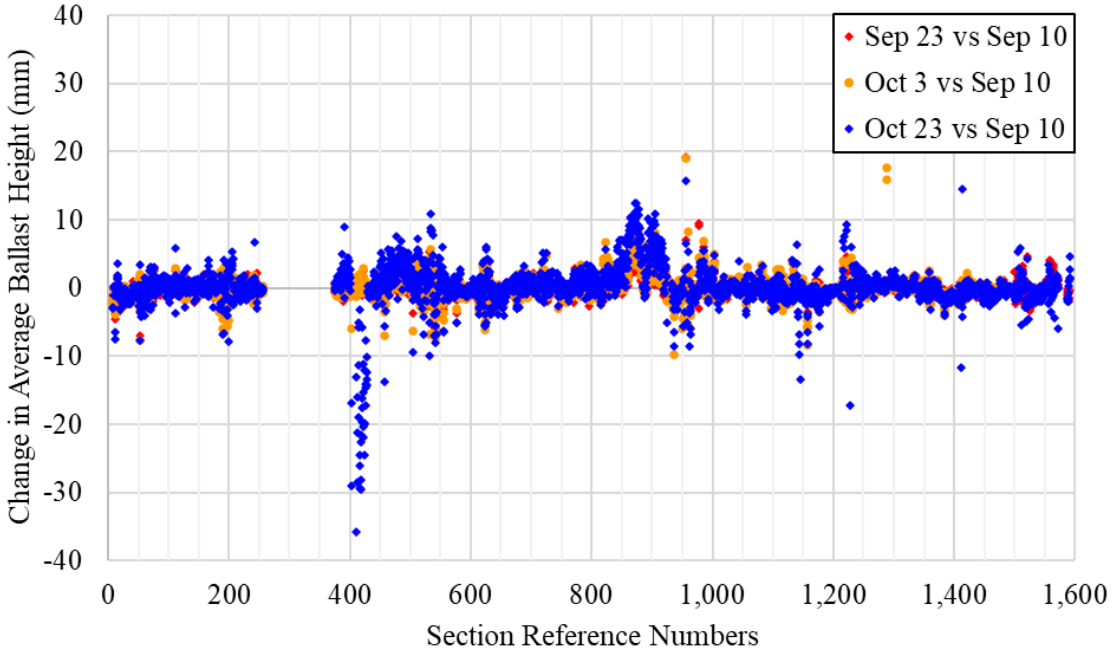

Figure 19. Crib Ballast Height Changes

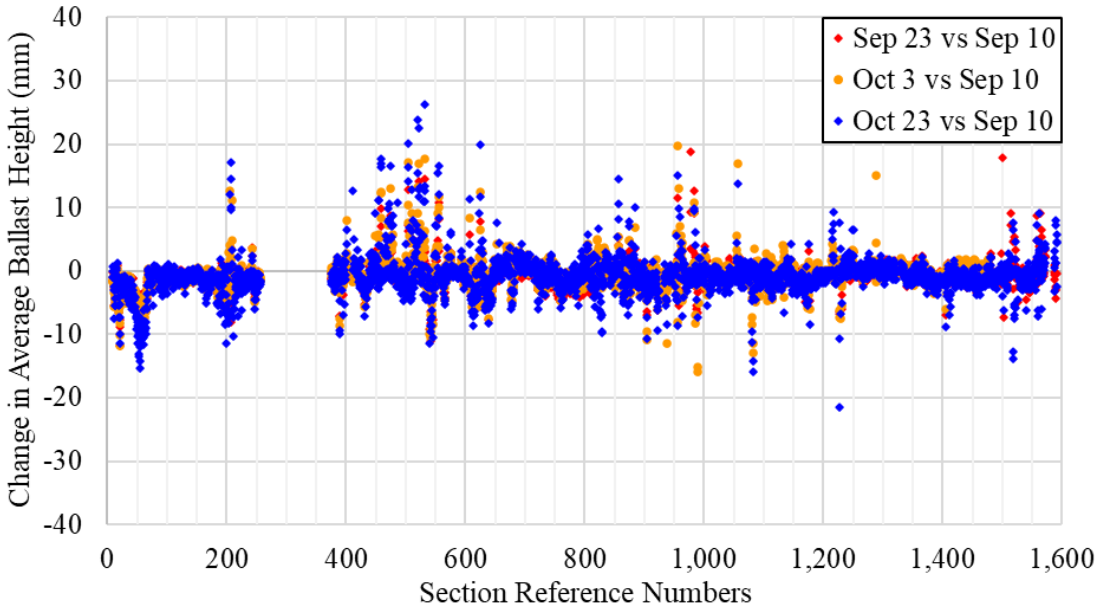

Figure 20. Right Ballast Height Changes

Crib ballast heights measured on September 10 versus those measured on October 23 are shown in Figure 21. Portions of the track with the most pronounced change are marked with relatively "warm" colors (e.g., yellow and red), while less significant changes have "cool" colors (e.g., purple and blue). There were numerous track locations with ballast level changes greater than 10 mm. The most detected changes were reductions in ballast levels, however, a few small increases occurred. The red circles highlight change locations that are detailed in the following paragraphs.

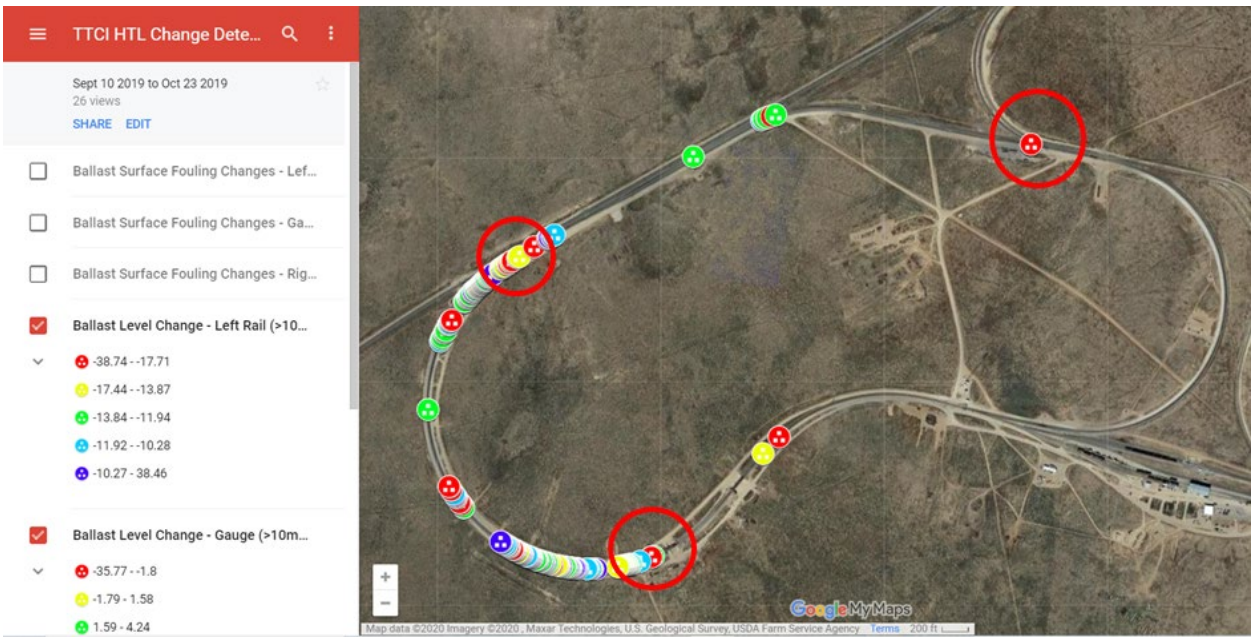

Figure 21. Ballast Height Changes per Meter of Travel (Sept. 10 vs. Oct. 23)

Figure 22 shows an example of ballast migration from the crib to the high rail shoulder using elevation-colorized 3D scan data (in LAS format). This example is from HTL sections 415 to 419. Colored areas reflect the height relative to the top of rail. Cooler colors are lower than warmer colors.

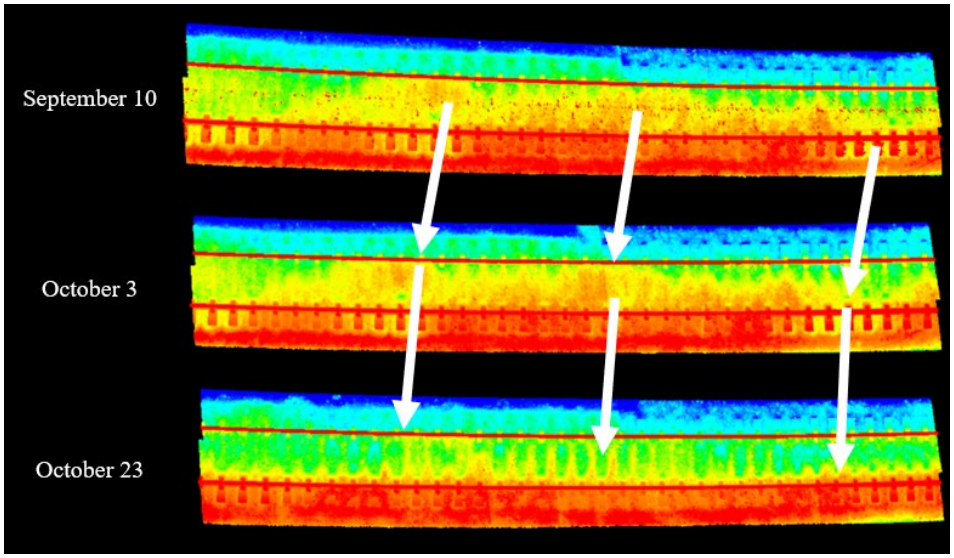

Figure 22. Ballast Level Changes between Sections 415 and 419

Figure 23 shows an example of a crib ballast level decrease between HTL sections 935 to 985. These data were also captured on a curve.

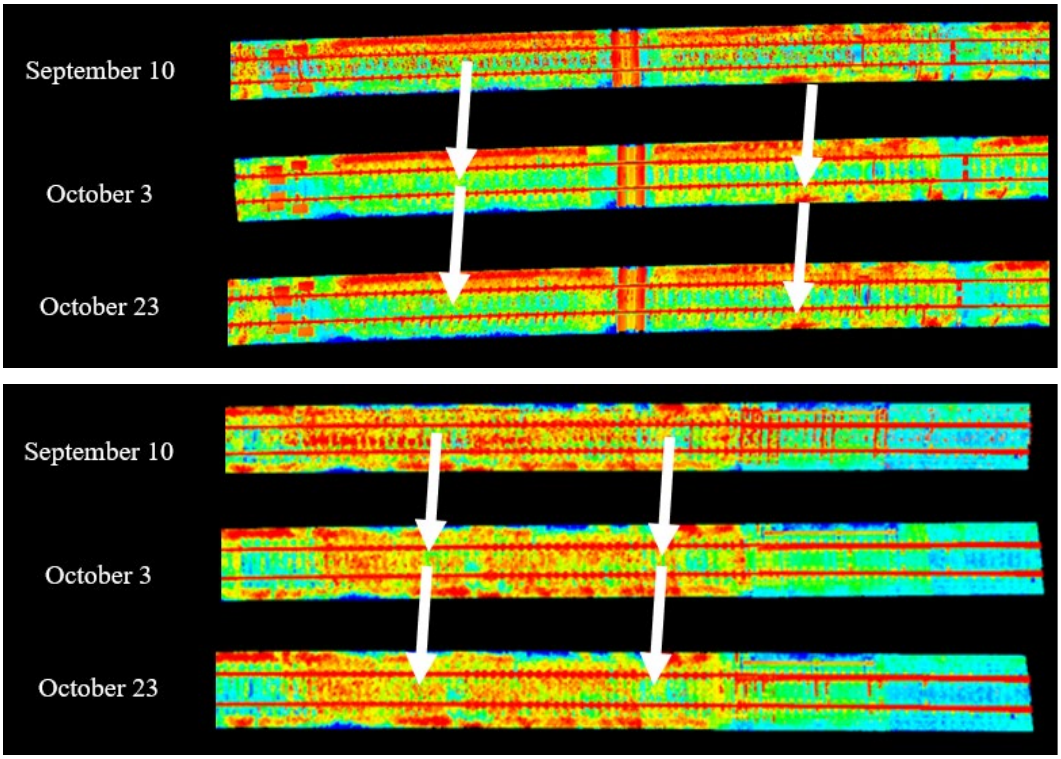

Figure 23. Ballast Level Changes between Sections 935 and 985

Figure 24 shows an example of a ballast level decrease followed by an increase between sections 1,500 and 1,520. The ballast level first decreased (note the shift toward blue pixels) between September 10 and October 3, then the ballast level increased (note the shift toward red pixels) between October 3 and October 23.

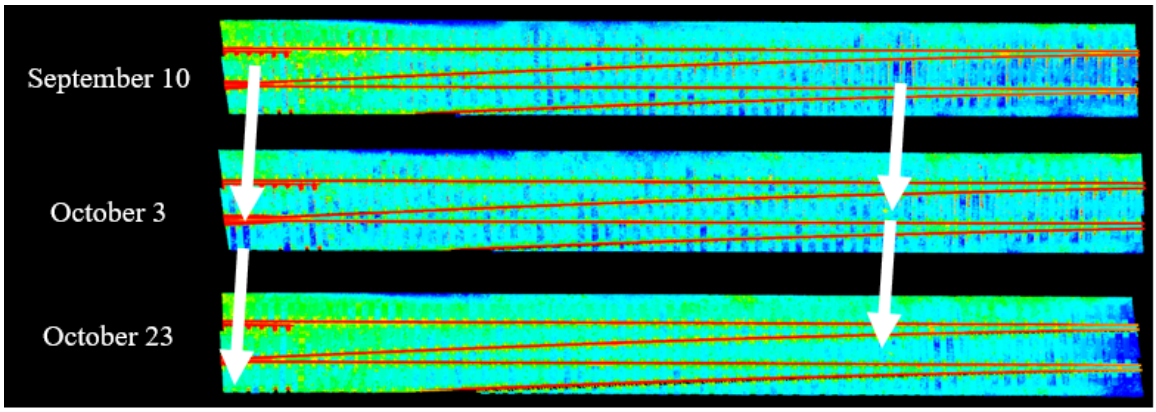

Figure 24. Ballast Level Changes between Sections 1,500 and 1,520

5.2 Ballast Surface Fouling Change Detection

Researchers trained the DCNN to detect and quantify surface fouling using human selected LRAIL range data image sets containing examples of fouled and clean ballast in track. . Like with ballast height change detection, the track analysis was divided into the crib (red) and shoulders (yellow), as shown in Figure 16. The change in ballast fouling is calculated as the difference in the amount of fouling present along 20 meters of track.

Figure 25, Figure 26, and Figure 27 present the run-to-run comparisons between three deployments: September 10 versus September 23, September 10 versus October 3, and September 10 versus October 23 – for the left shoulder, crib, and right shoulder, respectively, with the difference in ballast fouling plotted along the Y-axis and the location for each comparison plotted along the X-axis. Each point in the plot represents a change in ballast fouling. The track section between sections 260 and 360 contained a confidential experiment, thus no data exists for this portion.

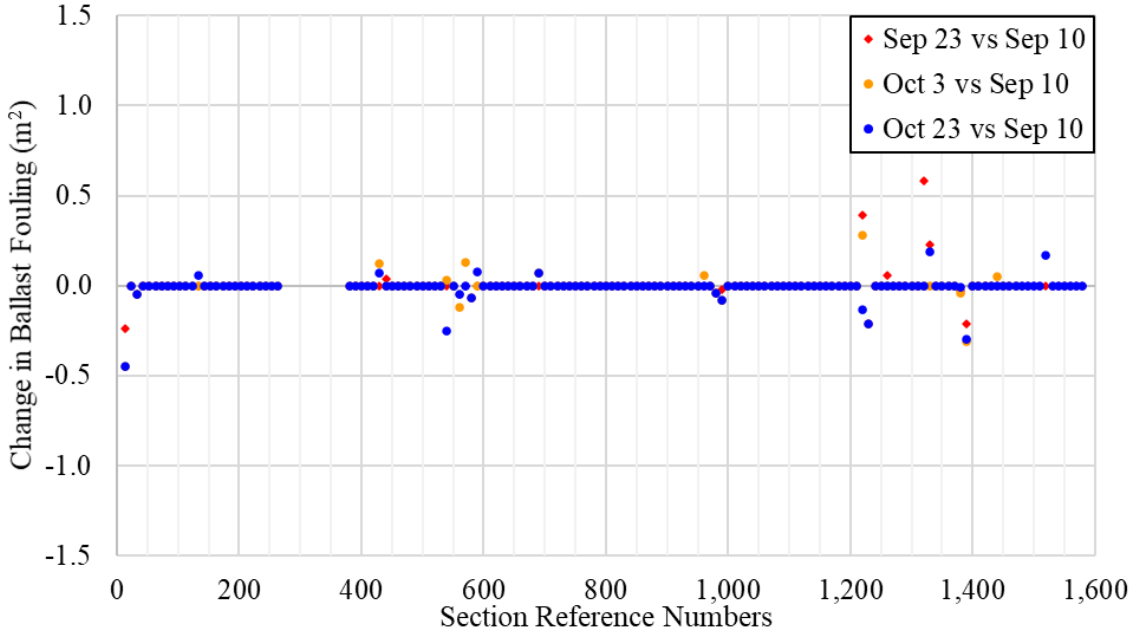

Figure 25. Left Ballast Fouling Area Change

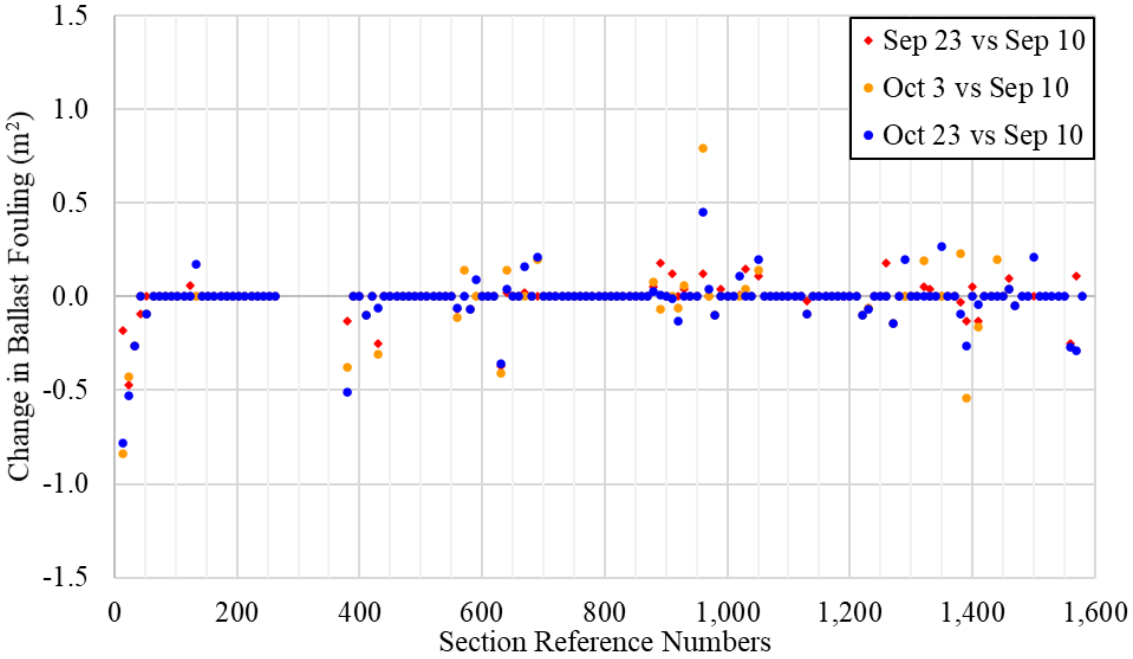

Figure 26. Crib Ballast Fouling Area Change

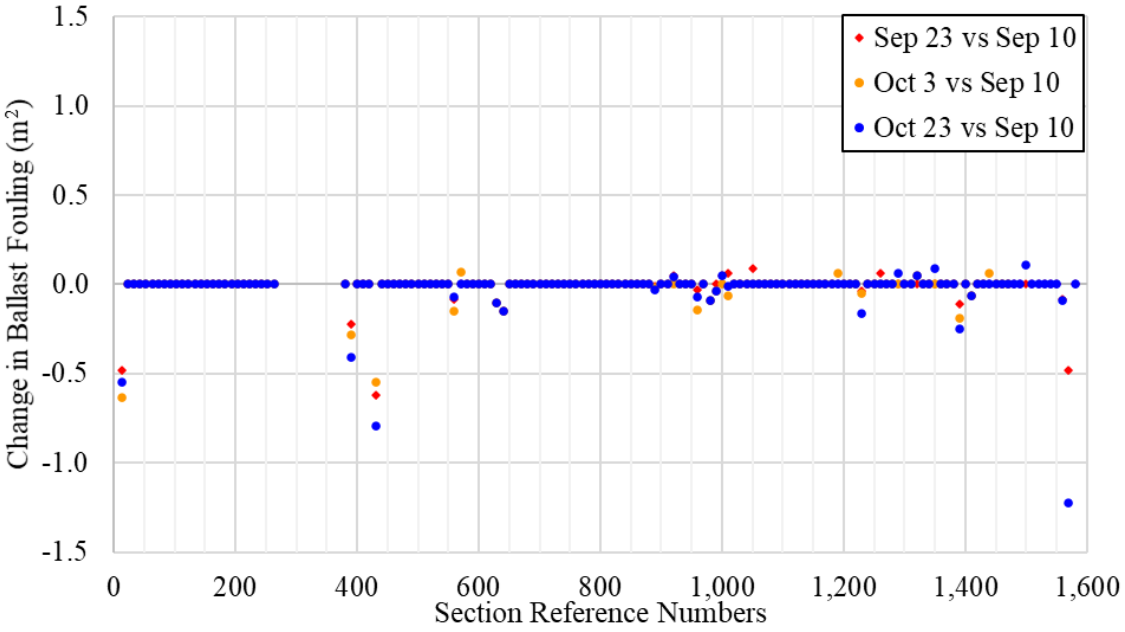

Figure 27. Right Ballast Fouling Area Change

Numerous changes in ballast fouling were detected. The locations of these changes between September 10 and October 23 are presented in Figure 28. The figure legend describes the use of relatively warm colors (e.g., yellow and red) to highlight track sections with higher measured change and cool colors (e.g., purple and blue) to highlight track sections with less significant change. The red circles highlight change locations that are detailed in the following paragraphs.

Figure 28. Ballast Fouling per 20-meter Track Length (Sept. 10 vs. Oct. 23)

Numerous track locations had fouling changes greater than 0.2 m^2. The predominant change was a decrease in ballast fouling, but there were some small increases as well.

Figure 29 presents an example of a detected change in of ballast fouling. The reduction of brown, highlighted ballast zones in the left and right shoulders represents the change.

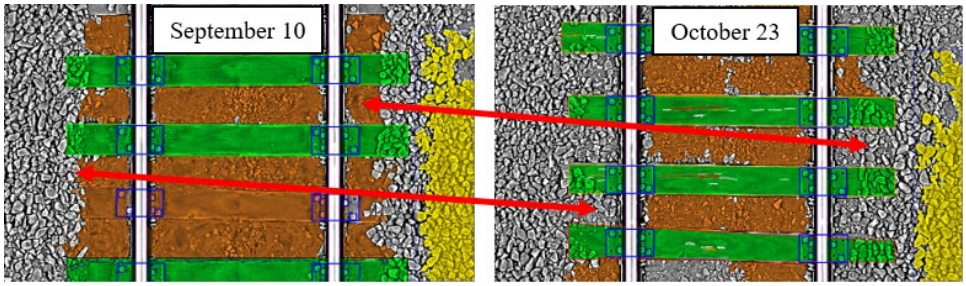

Figure 29. Ballast Fouling Reduction at Section 13

Figure 30 shows an example of a small reduction in ballast fouling. The reduction of brown, highlighted ballast zones in the crib and right shoulders represents this change.

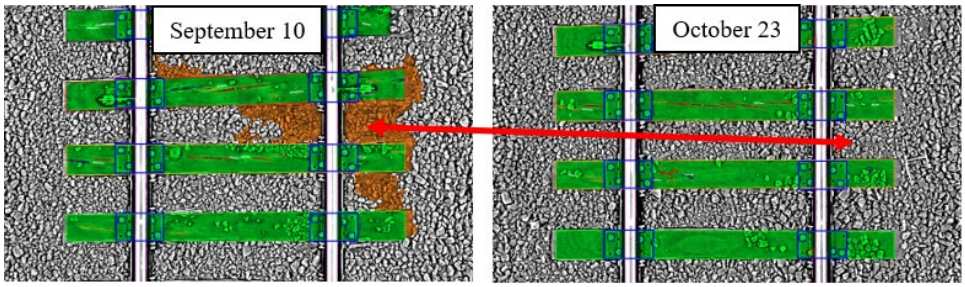

Figure 30. Ballast Fouling Reduction at Section 1,561

5.3 Crosstie Skew Change Detection

To detect changes in crosstie skew over time, run-to-run comparisons were made of the degree of crosstie skew angle (Figure 31).

Figure 31. Timber Crosstie Skew Example

Figure 32 presents the run-to-run comparison for crosstie skew angle between two datasets. Differences in measurements are along the Y-axis, and the location for comparison are along the X-axis. Each point represents a skew angle comparison (of magnitude greater than 0.5°) between runs for an individual crosstie. The track section between sections 260 and 360 contained a confidential experiment, thus no data were collected within this range. Bridges and special track work have zero values.

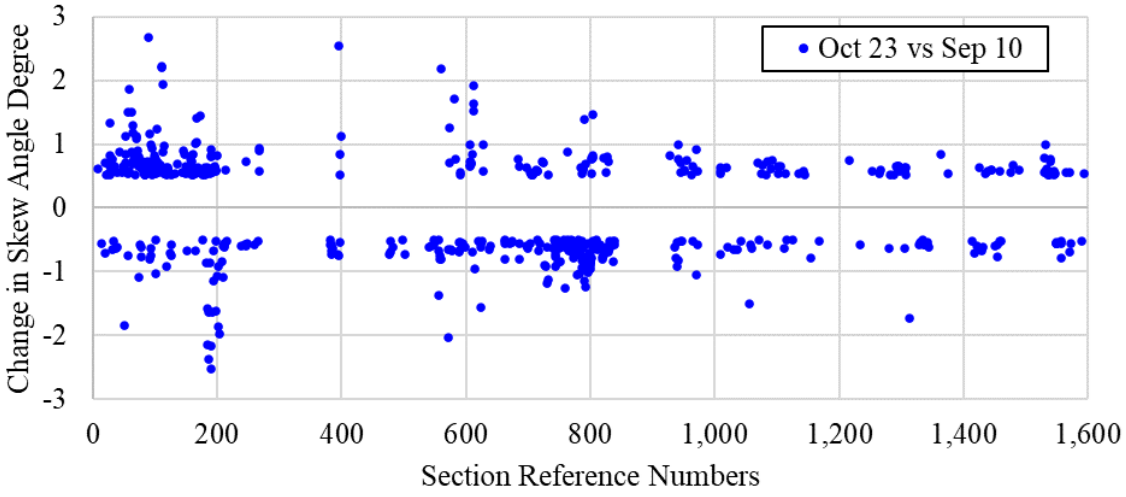

Figure 32. Change in Crosstie Skew

Figure 33 presents an example of a detected crosstie skew decrease. Figure 34 shows an example of a concrete crosstie skew increase.

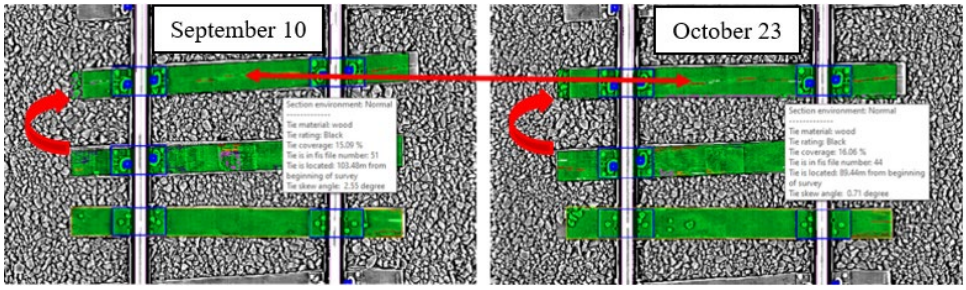

Figure 33. Example of Crosstie Skew Angle Decrease

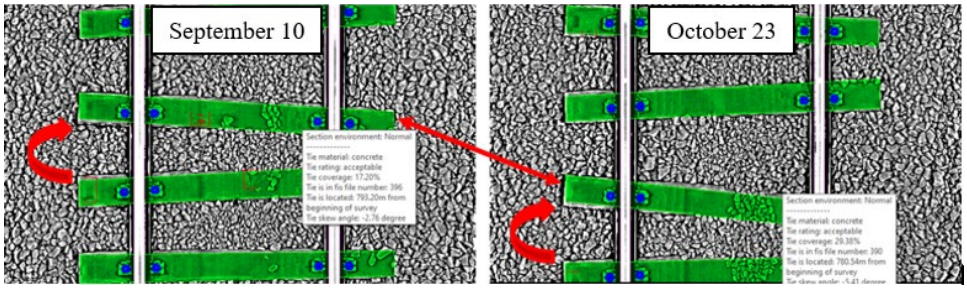

Figure 34. Example of Crosstie Skew Angle Increase

5.4 Crosstie Condition Change Detection

An algorithm automatically performed crosstie grading by analyzing timber crosstie 3D scans to detect and quantify cracking, splits, and holes in crosstie surfaces. Individual defects are grouped and color-coded according to severity (Figure 35 and Table 3). Additionally, an overall crosstie grade was assessed for each timber crosstie based on the aggregate defects (Table 4), with the bounding box of each timber crosstie highlighted using a different color to indicate its calculated grade. Crossties are grouped into acceptable or unacceptable categories based on their individual grades. Change is reported as run-to-run comparisons of the percentage of acceptable crossties per half-mile for both timber and concrete crossties.

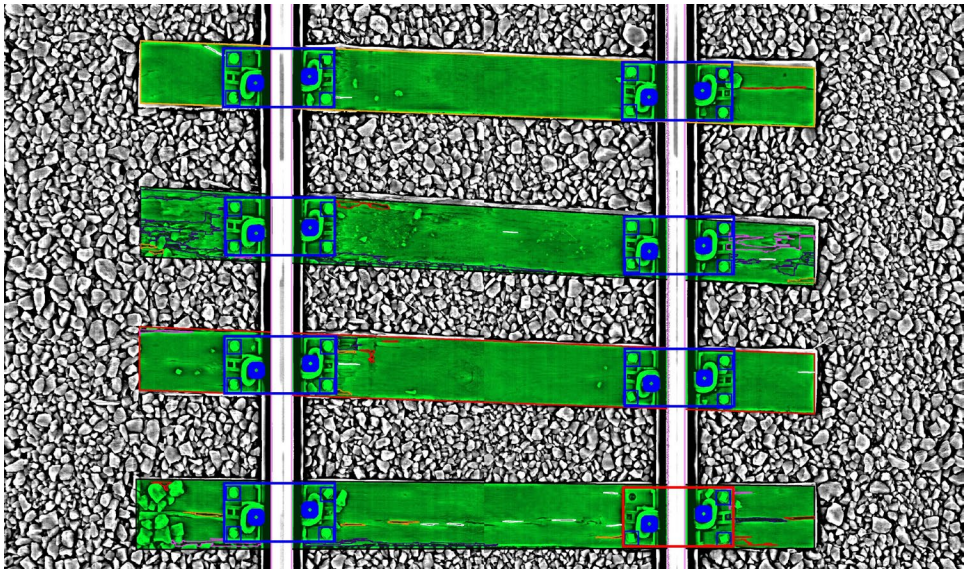

Figure 35. Timber Crosstie Showing Color-Coded Defects

Table 3. Crosstie Severity Rating for Individual Defects

Defect Colour	Depth	Width	Length
Very Severe	Defects in ties which contain ballast materials		
Severe	2 cm+	5 cm+	60 cm+
Moderate	1-2 cm	3-5 cm	15-60 cm
Light	Not considered	1-3 cm	10-15 cm
Very Light	Not considered	0.5-1 cm	Not considered
Unmarked	Not considered	Under 0.5 cm	Not considered

Table 4. Overall Crosstie Condition Score Based on Individual Defects

Tie Box Colour	Overall Tie Rating
D: Failed Tie	More than 3.7% of tie surface area contains ***Very Severe, Severe, Moderate or Light*** defects.
C: Near Failure Tie	Between 3.7% and 3.1% of tie surface area contains ***Very Severe, Severe, Moderate or Light*** defects.
B: Fair Condition Tie	Between 3.1% and 2.6% of tie surface area contains ***Very Severe, Severe, Moderate or Light*** defects.
A: Good Condition Tie	Any tie which does not fall into the 3 above categories.

For concrete crossties, spalls and cracks were detected first (Figure 36). Next, an overall condition was determined based on a combination of defect size and location. Like timber crossties, the DCNN used bounding boxes of different colors to indicate the overall grading of each concrete crosstie.

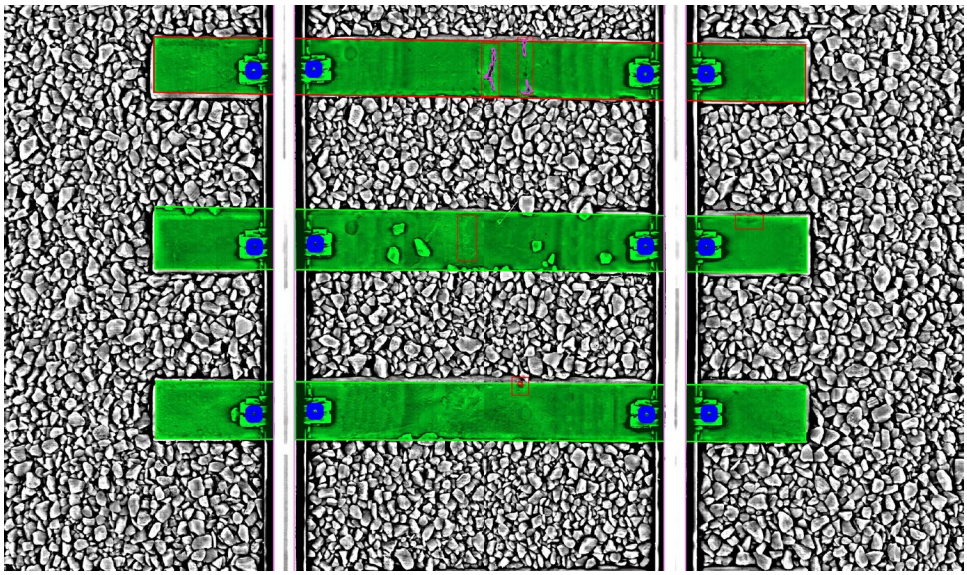

Figure 36. Intensity Image Showing Automatic Detection of Cracking and Spalling on Concrete Crossties

Following individual tie grading, the system grouped concrete crossties into two categories (acceptable and unacceptable), with the number of crossties falling into each category reported on a per half-mile basis. Figure 37. Change in Crosstie Condition shows the percentage of acceptable crossties per half-mile between runs, with the difference plotted along the Y-axis and the location for each comparison plotted along the X-axis.

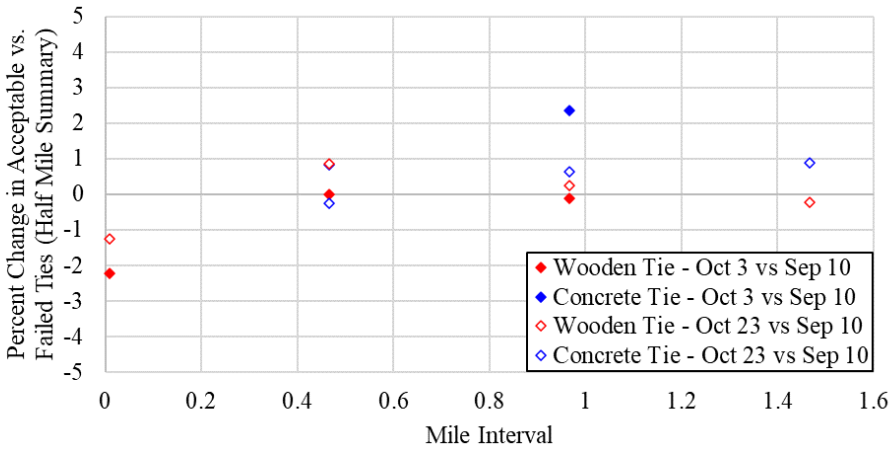

Figure 37. Change in Crosstie Condition

Given the project's relatively short duration, there was little detected change in crosstie condition. Change detection results were around 1 percent for each run-to-run comparison, with a maximum change of approximately 2 percent.

5.5 Joint Bar (and Welding Strap) Bolt Count and Joint Gap Change Detection

Change detection results included changes in joint presence, joint bar bolt count, and joint gap width between runs. The system was 100% reliable in detecting joint bars in track. Positive changes in bolt count indicated the installation of a new joint and/or additional bolts, while negative changes in bolt count indicated either the loss of bolts or the removal of a joint. Joint bar bolt counts from each of the five deployments were compared, with the difference in bolt count plotted along the Y-axis and the location of each comparison plotted along the X-axis (Figure 38).

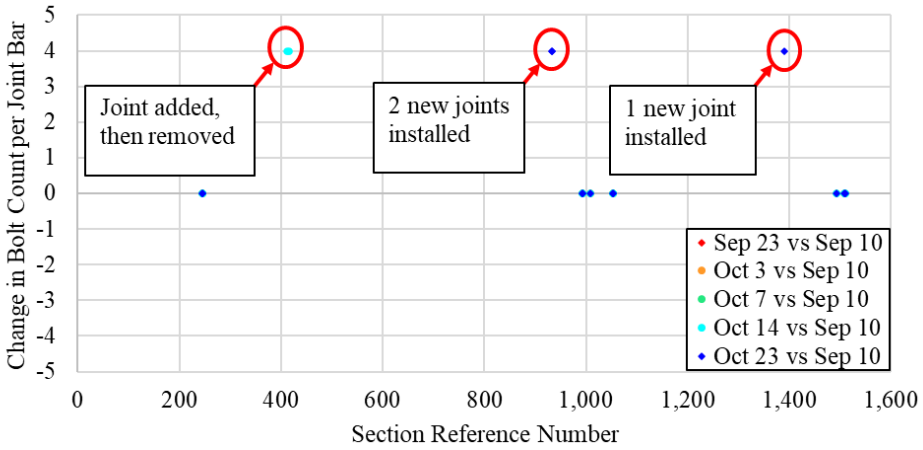

Figure 38. Changes in Bolt Count per Joint Bar

In total, four changes to joint bar bolt count were detected over the test period – one new joint (later removed) and three new joints. Two changes were found in section 933, where the rail was continuous on September 10 and September 23, but had two new joints installed before October 23 (Figure 39).

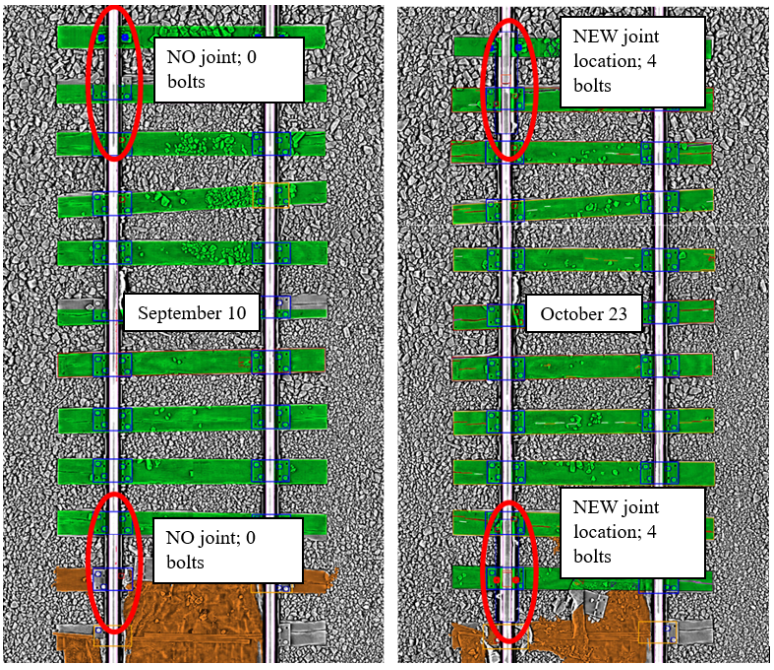

Figure 39. No Joint Bar (Left) and Two Joint Bars (Right)

The third change was found in section 1,390, where the rail was continuous on September 10, but had a new joint by October 23 (Figure 40).

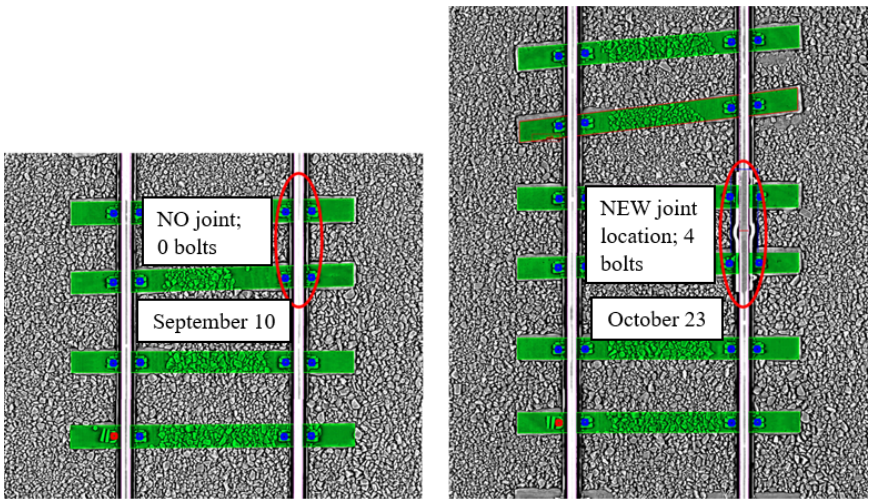

Figure 40. No Joint Bars (Left) and 1 Joint Bar (Right)

The fourth change was found in section 415. On September 10, the rail was continuous. Before October 3 a new joint had been installed on the left rail. The joint was removed by the October 23 inspection run (Figure 41).

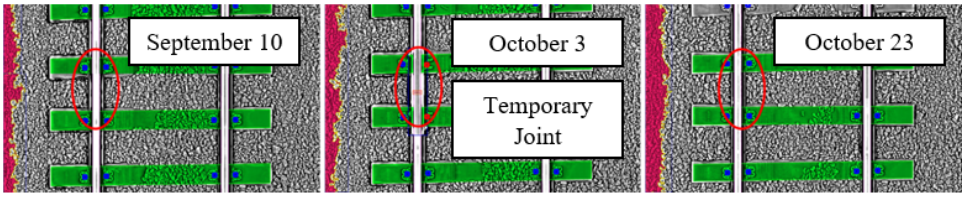

Figure 41. Joint Bar Only Present on October 3 (Center)

The system also analyzed the change in the joint gap width. Table 5 shows the changes in joint gap width for the 13 detected joints between September 10 and October 23.

Table 5. Joint Bar Gap Changes

Sept. 10 Section ID	Oct. 23 Section ID	Sept. 10 Joint Gap (mm)	Oct. 23 Joint Gap (mm)	Joint Gap Change
245	239	3.2	1	-2.2
246	240	1	3.5	2.5
994	990	1.8	2.1	0.3
1,054	1,050	1	2.2	1.2
1,510	1,507	4.1	1	-3.1
933	928	0	3.2	3.2
934	930	0	10.4	10.4
993	989	5.3	4.1	-1.2
1,009	1,005	1	2.3	1.3
1,054	1,050	1	1	0
1,493	1,490	2.3	1	-1.3
1,509	1,506	1.6	1	-0.6
1,390	1,387	0	0	0

Figure 42 shows the joint gap for section 245, and Figure 43 shows the joint gap for section 246.

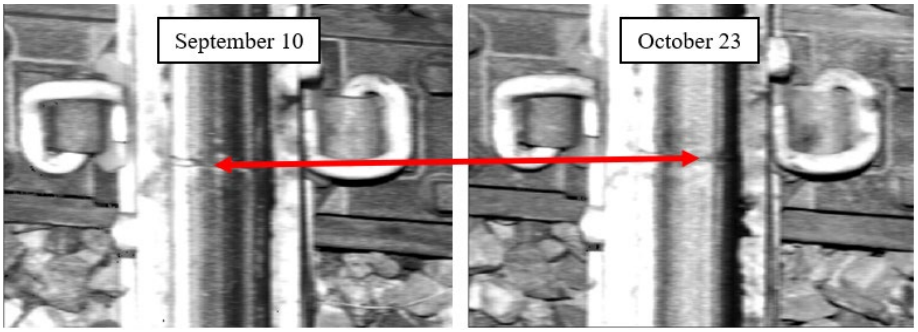

Figure 42. Original Joint Gap (Left) and Contracted Joint Gap (Right)

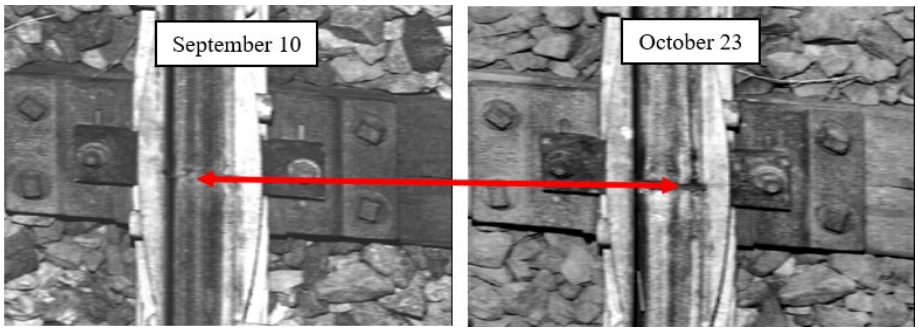

Figure 43. Original Joint Gap (Left) and Expanded Joint Gap (Right)

5.6 Elastic Fastener Status Change Detection

Elastic fastener status change detection involved run-to-run comparisons of the number of acceptable (present and properly seated/installed) fasteners versus unacceptable fasteners (missing or loose) (Figure 44). Each point on the graph represents a 10-meter length of track where the system detected three or more fastener changes. The number of fastener status changes are along the Y-axis, and the locations for these comparisons are along the X-axis. Positive instances indicate the addition of fasteners and/or the improvement of their installation between runs. Negative instances indicate the removal of fasteners and/or the loosening of fasteners between runs. Thus, a point reported at a value of two (2) on the Y-axis indicates a 10-meter stretch with at least six fasteners receiving an improvement in status (either newly installed or tightened).

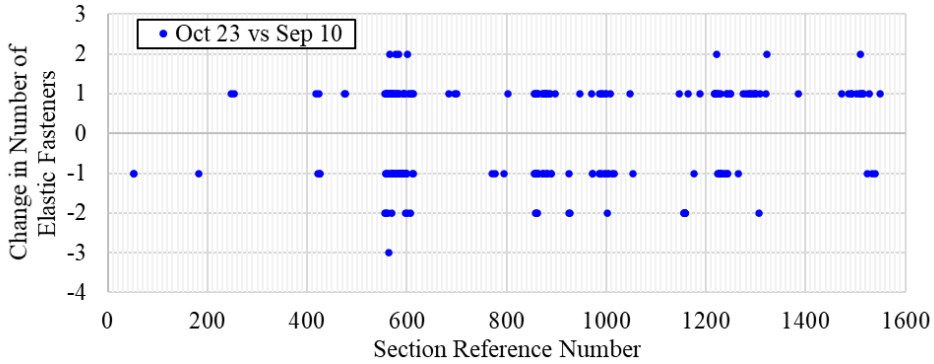

Figure 44. Change in Fastener Count

These results are summarized in Table 6 for September 10 versus October 3 and September 10 versus October 23, respectively.

Table 6. Threshold Fastener Changes (Sept. 10 vs. Oct. 3)

Approximate Beginning Section ID	Approximate Ending Section ID	Oct. 3 Number of Changes	Oct. 23 Number of Changes
411	412	3	-
423	425	3	4
569	571	3	-
571	584	-	7
608	613	4	4
859	865	3	-
925	928	-	4
971	972	-	3
1,156	1,159	19	20
1,219	1,230	-	7
1,280	1,308	12	11

Three of the change detection results from Table 6 are shown in Figure 45 and Figure 46. Figure 45 illustrates the system correctly identifying a fastener that changed from absent or covered to present or visible.

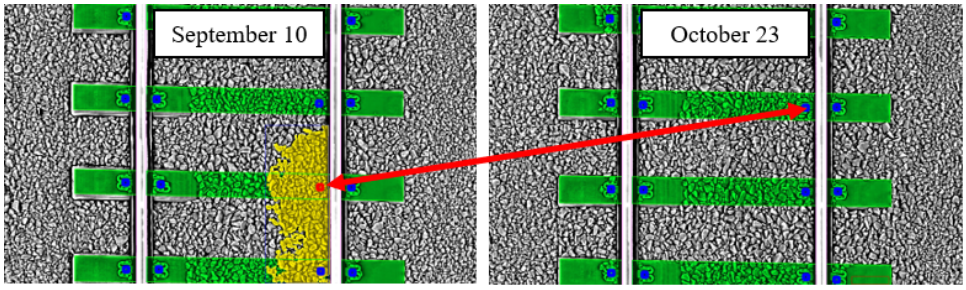

Figure 45. First Fastener Change Identification

Figure 46 illustrates the detection of two fastener changes.

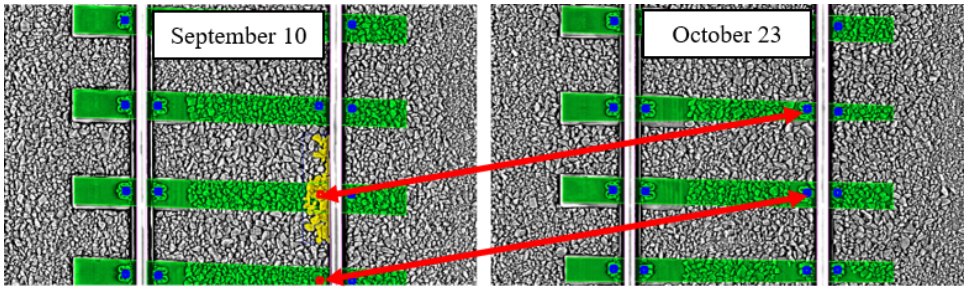

Figure 46. Second and Third Fastener Change Identification

5.7 Spike Height Change Detection

Spike height changes between runs were analyzed on a region of interest (ROI) basis, instead of spike-to-spike, to report changes with sufficient magnitude to be of interest to railroad operators. Four spike ROIs were defined for each tie (two per rail) and the mean spike height calculated for

each ROI (based on the spike heights in the given ROI). To detect changes in spike height between runs, a mean spike height statistic was automatically calculated for each of the four ROIs on each crosstie (Figure 47). The system reported changes in the mean spike height in each ROI between runs.

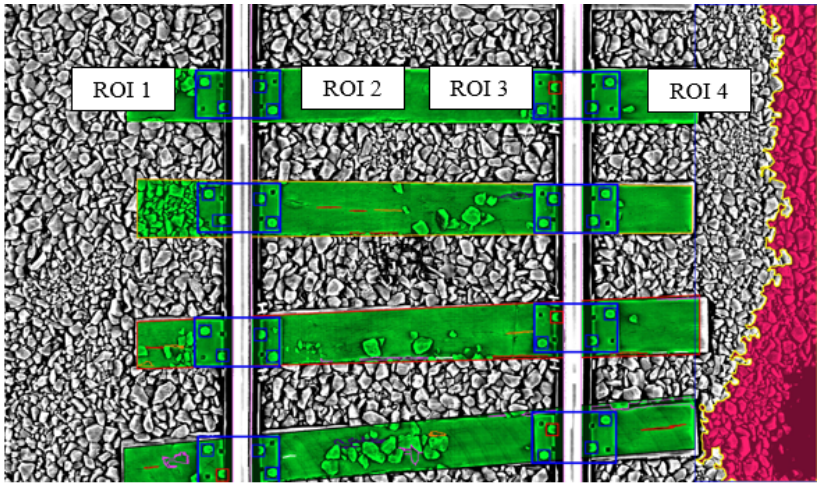

Figure 47. Spike Height ROIs

Figure 48, Figure 49, Figure 50, and Figure 51 show the run-to-run comparisons of September 10 (first deployment) versus October 23 (last deployment) for the four ROIs. The differences in spike height are plotted on the Y-axis, and the location for each comparison are along the X-axis. Each point represents a change in mean spike height within a single ROI. Section number gaps indicate areas that were either confidential (no data recorded) or did not have fastening systems with spikes (e.g., concrete crossties).

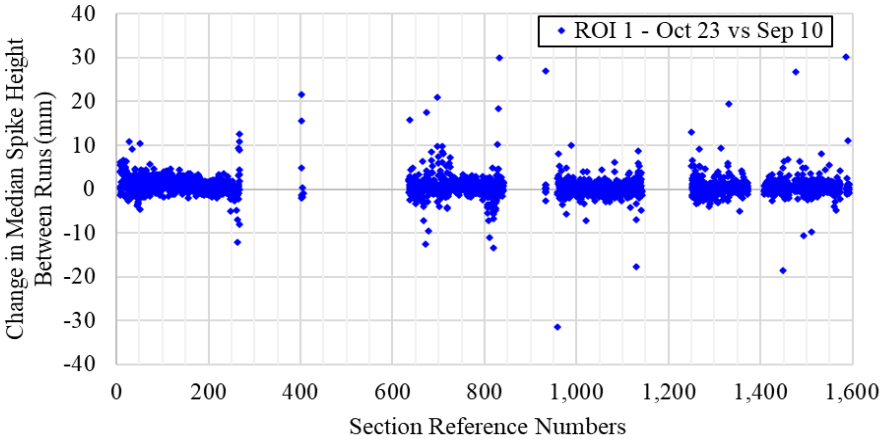

Figure 48. ROI 1 Spike Height Changes with Respect to Baseline Run (Sept. 10)

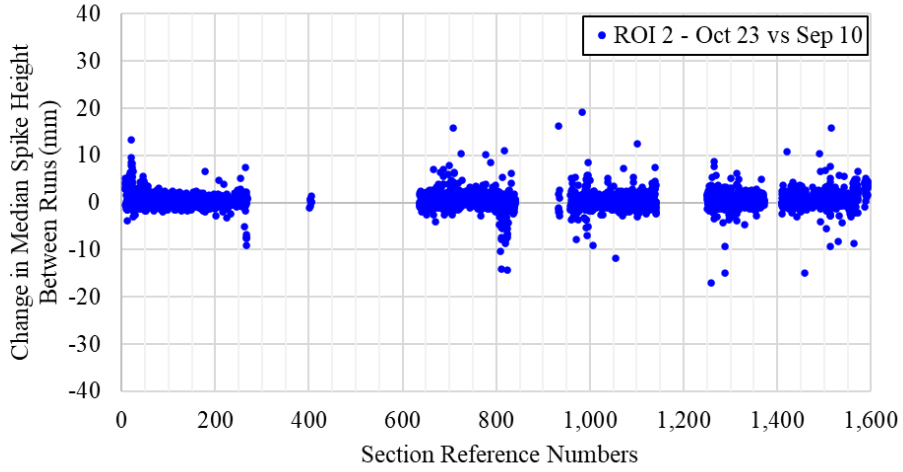

Figure 49. ROI 2 Spike Height Changes with Respect to Baseline Run (Sept. 10)

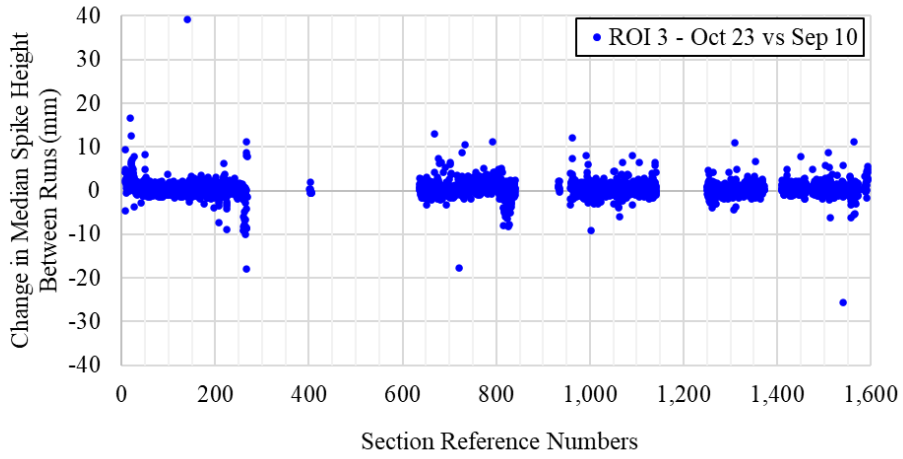

Figure 50. ROI 3 Spike Height Changes with Respect to Baseline Run (Sept. 10)

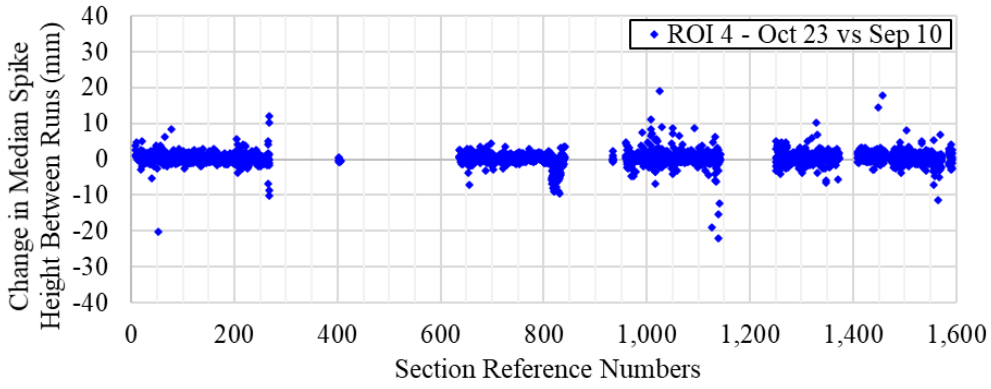

Figure 51. ROI 4 Spike Height Changes with Respect to Baseline Run (Sept. 10)

Figure 52 shows an example of a large spike height increase in ROI 1 with a 19-mm increase between September 10 and October 23.

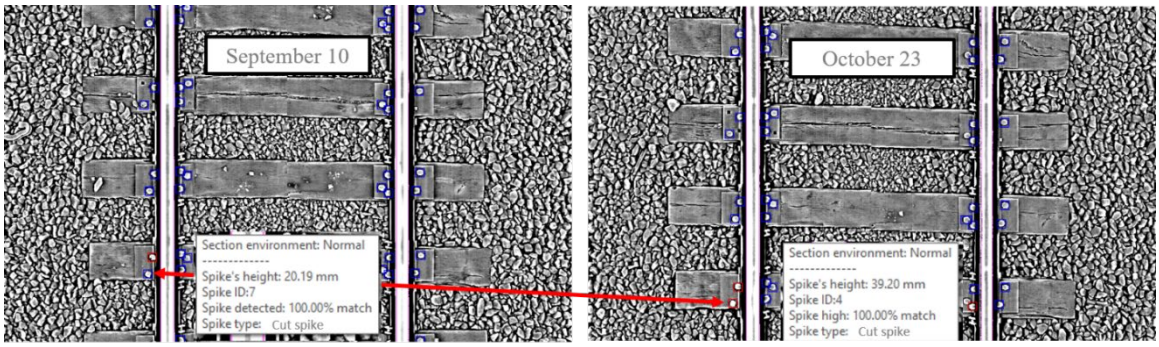

Figure 52. Spike Height Increase in ROI 1

Figure 53 shows an example of a large spike height decrease in ROI 2 with a 15-mm reduction between September 10 and October 23.

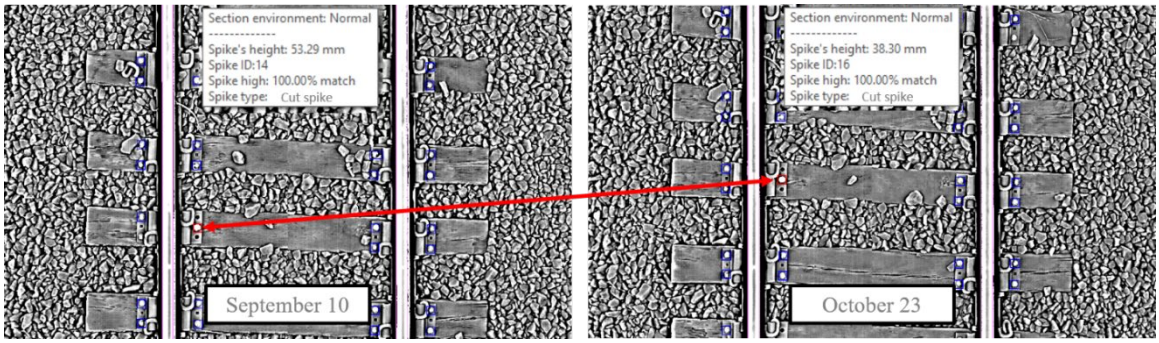

Figure 53. Spike Height Decrease in ROI 2

6. Conclusion

Illinois and Railmetrics, Inc. successfully evaluated the use of 3D LRAIL, DCNNs, and change detection technology for railway track safety inspections. This combination of technologies can provide value-added inspection data to traditional track inspection methods. The potential of this new technology to augment and improve traditional human track inspection activities has been established.

6.1 Accuracy and Precision

The project team completed extensive DCNN training using a wide variety of track system features from the HTL at TTC. Feature extraction and classification maturity of the DCNN were greatly enhanced over the course of this project. Specifically, the team validated DCNN performance with a human-in-the-loop check of the DCNN. The percent agreement between the DCNN and a human evaluator reached 99 to 100 percent for both elastic fasteners and spikes, exceeding the target of 75 percent.

6.2 Component and Condition Recognition

The research team used features and classifiers as inputs to an automated track change detection algorithm. Change detection proved sensitive to various features and conditions. In doing so, change detection analysis using DCNN results as inputs was also successfully demonstrated across a wide variety of track conditions and parameters, including ballast level, ballast fouling, joint bar bolting, joint bar gap, fastener and spike presence and condition, and crosstie skew and condition (Table 7).

Table 7. Change Detection Results Summary

Region of Interest	Reporting Metric (Summary from Table 1)	Summary of Outcome
Shoulder ballast	Significant changes in average level relative to top of rail within a crib and shoulder areas or along a stretch of track; changes in fouling (presence of non-ballast materials); changes in the presence of surface water or moisture	Changes in shoulder ballast level and fouling successfully detected.
Crib ballast	Significant changes in average level relative to top of rail; changes in fouling (presence of non-ballast materials); changes in the presence of water or moisture	Changes in crib ballast level and fouling successfully detected.
Field and gauge-side fastener areas	Significant changes in present fastener counts per km as a percentage; significant changes in the position of multiple fasteners	Changes in spike height and presence and fastener features and presence successfully detected.
Crosstie ends and centers	Significant changes to individual ratings of crossties per km; significant changes to skew angle of multiple crossties	Tie skew changes successfully detected, although there was not enough change between deployments for successful crosstie change evaluation.
Joint bars	Significant changes to joint bolting and joint bar gap	Joint bar bolting and gap width successfully detected.

6.3 Advancement of Change Detection Technology

This research demonstrated encouraging progress in automating the track inspection process to improve both the safety and efficiency of rail operations. It can detect subtle changes and goes beyond the traditional pass/fail approach to meet maintenance and safety thresholds.

Overall, the project results increased the technology readiness level of ATCD from technology readiness level TRL6 to TRL7 by demonstrating the prototype in a relevant operational environment (HTL at TTC). With sample size increases from revenue service track deployments, these DCNNs could advance the system to a commercially viable state.

7. Future Research

The successful outcome of this project should inspire future work. Such work would require collaboration with a Class I railroad for access to infrastructure and to obtain revenue service change detection data.

7.1 Development of Condition Change Index

The research team first recommends the development of a meaningful method for reporting change data by way of a condition change index. This index would facilitate quantification of how changes in certain track features influence track strength and safe train operations.

7.2 Revenue Service Track Deployment

The research team recommends the continued development and testing of automated track change detection technology on revenue service track. Testing on a wide variety of track types will improve the performance of DCNN feature and classification algorithms by adding more variety to the feature training models. Additionally, revenue service testing presents an opportunity to further evaluate system repeatability and would allow researchers to evaluate the DCNN's performance with differing environmental conditions.

7.3 Comparison to Traditional Geometry Data

Revenue service field data will support the development of relationships between automated track change detection and other track inspection technologies (e.g., TGMS, GRMS, etc.). The comparison of these data types will allow the study of precursor relationships that may exist between track feature changes and resulting changes in discrete measurement data produced by traditional inspection systems. Such research will lead to higher quality information to assist with preventative maintenance activities.

7.4 Development of Business Rules

The research team proposes working directly with practitioners to establish business rules for change reporting that can provide value for both routine track inspection and maintenance planning activities. This is consistent with broader trends in the industry directed toward using track condition and performance data as an input to capital maintenance planning activities.

8. References

[1] Federal Railroad Administration (March 2018). Track and Rail and Infrastructure Integrity Compliance Manual: Volume I - Chapter 2 - Field Reporting Procedures and Forms. March 2018.

[2] Georgetown Rail Equipment. Aurora XivTM.

[3] Orrell, S. C., Nagle, J. A., & Christopher, V. (November 2009). System and Method for Inspecting Railroad Track. United States Patent US 7.616,329 B2.

[4] Berry, A., Gibert-Serra, X., McNew, D., & Nejikovsky, B. (2008). High Speed Video Inspection of Joint Bars Using Advanced Image Collection and Processing Techniques. *World Congress on Railway Research.* Seoul.

[5] bvSys Bildverarbeitungssysteme GmbH. Railcheck.

[6] MERMEC Group. Rail Corrugation; V-Cube.

[7] Pavemetrics. Laser Rail Inspection System (LRAIL).

[8] Schmidhuber, J. (January 2015). Deep Learning in Neural Networks: An Overview. *Neural Networks, 61*, 85-117.

[9] Chen, J., Liu, Z., Wang, H., Nunez A., & Han, Z. (2018). Automatic Defect Detection of Fasteners on the Catenary Support Device Using Deep Convolutional Neural Network. *IEEE Transactions on Instrumentation and Measurement, 67*(2), 257-269.

[10] Faghih-Roohi, S., Hajizadeh, S., Nunez, A., Barbuska, R., & De Schutter, B. (2016). Deep convolutional neural networks for detection of rail surface defects. *2016 International Joint Conference on Neural Networks (IJCNN).* Vancouver.

[11] Wei, X., Yang, Z., Liu, Y., Wei, D., Jia, L., & Li, Y. (2019). Railway track fastener defect detection based on image processing and deep learning techniques: A comparative study. *Engineering Applications of Artificial Intelligence, 80*, 66-81.

[12] Giben, X., Patel, V. M., & Chellappa, R. (2015). Material classification and semantic segmentation of railway track images with deep convolutional neural networks. *2015 IEEE International Conference on Image Processing (ICIP).* Quebec City.

[13] Chellappa, R., Xavier, G., & Vishal, P. (June 2015). Robust Anomaly Detection for Vision-Based Inspection of Railway Components (Report No. DOT/FRA/ORD-15/23). Federal Railroad Administration.

[14] Henderson, H. & Borsholm, A. (July 2019). Demonstration of Commercial-Off-The-Shelf Change Detection on Railway Images (Report No. DOT/FRA/ORD-19/22). Federal Railroad Administration.

[15] Fox-Ivey, R., Nguyen T., & Laurent, J. (March 2020). Laser Triangulation for Track Change and Defect Detection (Report No. DOT/FRA/ORD-20/08). Federal Railroad Administration.

[16] Fox-Ivey, R., Nguyen, T., & Laurent, J. (April 2020). Extended Field Trials of LRAIL for Automated Track Change Detection (Report No. DOT/FRA/ORD-20/14). Federal Railroad Administation.

[17] Transportation Technology Center Inc. High Tonnage Loop (HTL/FAST).

[18] Agresti, A. (2007). An introduction to categorical data analysis. 2nd ed., Hoboken: Wiley-Interscience.

Abbreviations and Acronyms

ACRONYM	DEFINITION
2D	Two Dimensional
3D	Three Dimensional
AI	Artificial Intelligence
CN	Canadian National Railroad
DCNN	Deep Convolutional Neural Network
FAST	Facility for Accelerated Service Testing
FRA	Federal Railroad Administration
HTL	High Tonnage Loop
LRAIL	Laser Rail Inspection System
LAS	3D Point Cloud File
mAP	Mean Average Precision
RailTEC	Rail Transportation and Engineering Center
RPN	Region Proposal Network
TTC	Transportation Technology Center